Soil Biology and Biochemistry 149 (2020) 107862

Contents lists available at ScienceDirect

Soil Biology and Biochemistry

journal homepage: http://www.elsevier.com/locate/soilbio

Changes in microbial community composition, activity, and greenhouse gas production upon inundation of drained iron-rich peat soils

Anniek E.E. de Jong [a,b,*], Simon Guererro-Cruz [a,1], Josepha M.H. van Diggelen [c], Annika Vaksmaa [a,2], Leon P.M. Lamers [d], Mike S.M. Jetten [a,b,e], Alfons J.P. Smolders [c,d], Olivia Rasigraf [a,f]

[a] Department of Microbiology, Institute for Water and Wetland Research, Radboud University, Heyendaalseweg 135, 6525, AJ, Nijmegen, the Netherlands
[b] Netherlands Earth Systems Science Center, Utrecht University, Heidelberglaan 2, 3584, CS, Utrecht, the Netherlands
[c] Research Centre B-WARE, Toernooiveld 1, 6525, ED, Nijmegen, the Netherlands
[d] Department of Aquatic Ecology and Environmental Biology Institute for Water and Wetland Research, Radboud University, Heyendaalseweg 135, 6525, AJ, Nijmegen, the Netherlands
[e] Soehngen Institute of Anaerobic Microbiology, Radboud University, Heyendaalseweg 135, 6525, AJ, Nijmegen, the Netherlands
[f] GFZ German Research Centre for Geosciences, Geomicrobiology section, Telegrafenberg, 14473, Potsdam, Germany

ARTICLE INFO

Keywords:
Restoration of drained peatlands
Methanogenesis
Microbial diversity
Methane
Nitrogen
Greenhouse gas emissions

ABSTRACT

Globally, large-scale land drainage has severely deteriorated the functioning and services of peatlands, making restoration plans of the utmost importance. Rewetting is essential for the restoration of drained peatlands, but the level of success including greenhouse gas (GHG) mitigation largely depends on the soil microbiome interactions under the prevailing biogeochemical conditions. Here, we investigated the effects of inundation of drained iron (Fe) -rich peat topsoils on nutrient release, surface water quality, GHG production and consumption, and on the composition and activity of the microbial community. The effect of the addition of different potential electron acceptors on methane (CH_4) production and consumption were studied in incubation experiments. In response to inundation, porewater concentrations of Fe, total inorganic carbon, ammonium, and phosphorus increased. CH_4 emissions increased in the control (i.e. without any additions) and Fe(III) oxide amended incubations upon inundation. This could be explained by the increase in the relative abundance of methanogens even though Fe(III) was previously hypothesized to lower methanogenic activity. In contrast, nitrite, nitrate, and sulfate-rich incubations inhibited methanogenesis. The prolonged exposure to nitrogen oxides stimulated denitrification with nitrous oxide (N_2O) as the main gaseous product, together with an increase in the relative abundance of denitrifying microorganisms. Our results demonstrate that insights into the changes in microbial communities in relation to soil geochemistry explain differences in responses observed in different peat soils observed upon inundation. The increase in emissions of the potent GHGs CH_4 and N_2O from Fe-rich peat topsoils are a major adverse effect in the early stage of inundation.

1. Introduction

Widespread drainage is compromising the capacity of the world's peatlands to serve as sinks for nutrients and carbon (C) (Lamers et al., 2015). During the first half of the 20th century, large areas (worldwide approximately 15%) of peatlands have been lost due to drainage, thereby enhancing the aerobic decomposition of organic matter (OM) (Joosten, 2010; Joosten and Clarke, 2002). As a result, drained peatlands have become net C sources, with an annual global emission of approximately 2 Gt carbon dioxide (CO_2). This is around 5% of all anthropogenic greenhouse gas (GHG) emissions originating from only 0.3% of the global land surface (Joosten et al., 2016). Simultaneously,

* Corresponding author. Department of Microbiology, Institute for Water and Wetland Research, Radboud University, Heyendaalseweg 135, 6525, AJ, Nijmegen, the Netherlands.
E-mail address: dejonganniek@gmail.com (A.E.E. de Jong).
[1] Present address: Global Center of Expertise in Microbiology & Adventitious Viral Agents Merck, CQ building, PO Box 20, 5340 BH Oss, The Netherlands.
[2] Present address: Department of Marine Microbiology and Biogeochemistry, NIOZ Royal Netherlands Institute for Sea Research and Utrecht University, Landsdiep 4, 1790 AB Den Burg, Texel, The Netherlands.

https://doi.org/10.1016/j.soilbio.2020.107862
Received 23 October 2019; Received in revised form 15 January 2020; Accepted 17 May 2020
Available online 22 June 2020

Fig. 1. Map indicating the location of the four sampled agricultural fields in The Netherlands. Map was created with GIS software.

this drainage has also caused severe land subsidence (2–150 mm yr^{-1}, depending on the region) (Leifeld et al., 2011; Syvitski et al., 2009), which may lead to high costs for infrastructure and, together with the anticipated sea-level rise, poses a severe inundation risk to often highly populated riverine areas and coastal deltas.

To counteract subsidence and restore ecosystem services, large areas of drained peatlands are being rewetted to restore the hydrology to historic water levels (Geurts et al., 2019). Although the positive effect of rewetting on carbon sequestration is undisputed, there are also several studies suggesting that there may be a considerable amount of CH_4 released after rewetting (Franz et al., 2016; Günther et al., 2019; Hahn et al., 2015; Harpenslager et al., 2015; Hemes et al., 2018; Knox et al., 2015; Vanselow-Algan et al., 2015; Wilson et al., 2009). In addition, nitrous oxide (N_2O) emission may increase due to denitrification of accumulated nitrogen oxides (Beare et al., 2009; Harrison-Kirk et al., 2013; Liu et al., 2018; Snider et al., 2015). Since the global warming potential of CH_4 is about 34 and N_2O is 298 times higher than that of CO_2 over 100 years (Myhre et al., 2013), rewetting could have an (initial) negative effect on the GHG emissions. The evolution of GHG emission patterns following rewetting can vary substantially (from years to decades) depending on previous land use, restoration methods applied, and local climate conditions (Baird et al., 2013; Beetz et al., 2013; Juottonen et al., 2012; Mohamed Abdalla et al., 2016; Samaritani et al., 2011; Strack and Zuback, 2013; Wen et al., 2018).

The shift in the GHG emissions is triggered by the large changes in the composition and activity of the microbial community upon rewetting. The increase in water table lowers the oxygen (O_2) concentrations in the formerly drained soil, thereby stimulating anaerobic microbial processes. OM will be decomposed in an anaerobic syntrophic food chain ultimately providing hydrogen, CO_2, and acetate to methanogenic archaea (Kotsyurbenko et al., 1993; Schink, 1997). The produced CH_4 will diffuse upwards in the soil column. A fraction of that CH_4 can then be oxidized by anaerobic methanotrophs to CO_2 under anoxic conditions using several alternative electron acceptors including nitrite (NO_2^-), nitrate (NO_3^-), sulfate (SO_4^{2-}), or iron (Fe) (III) oxides (Bhattacharjee et al., 2016; Boetius et al., 2000; Cai et al., 2018; Chang et al., 2012; Crowe et al., 2011; Egger et al., 2015; Ettwig et al., 2016, 2010; Haroon et al., 2013; Milucka et al., 2012; Raghoebarsing et al., 2006; Saunois et al., 2016; Scheller et al., 2016; Torres et al., 2014; Vaksmaa et al., 2017, 2016). CH_4 ultimately reaches oxic zones in the soil where it can be converted to CO_2 by aerobic methane oxidizing bacteria (MOB) (Semrau et al., 2010). Depending on the prevailing conditions, residual CH_4 can also escape biological oxidation and will be emitted to the atmosphere (Dean et al., 2018).

In order to establish optimal management strategies for peat restoration, the microbial processes governing the increase of CH_4 emissions upon rewetting need to be better understood. The microbial community composition and interactions controlling the fluxes of GHGs will be directly influenced by factors such as water table levels, presence of oxidizing agents (e.g. Fe(III) oxides and SO_4^{2-}) that have accumulated during years of oxic conditions in the soil vegetation productivity, soil temperature, and presence of labile carbon (Dean et al., 2018). The aim of our research was to study the effect of ecosystem relevant electron acceptors (NO_2^-, NO_3^-, SO_4^{2-}, Fe(III) oxides) on the microbial community composition and fluxes of CH_4 and N_2O in anaerobic incubations of inundated soils. Previous field studies showed that inundation of Fe-rich peat soils still may result in high CH_4 emissions, despite the predicted inhibition of methanogenesis at the presence of Fe(III) oxides (Bodegom

Table 1
Locations and properties of the four sampled soils. Total iron (Fe) and phosphorus (P) are in mmol kg dry weight^{-1}, the bulk density is in kg dry weight L^{-1} soil, and OM (organic matter content) is given in %.

Soil	Location	Latitude	Longitude	OM	Total Fe	Total P	Bulk density	Texture
IRS1	Abcoude	52.266	4.954	27	435	61	0.52	clayey peat
IRS2	Oude water	52.002	4.847	40	641	95	0.40	peat
IRS3	Wilnis	52.166	4.900	49	1691	119	0.37	peat
IPS	Loosdrecht	52.192	5.135	6.4	51	26	1.20	sandy peat

et al., 2004; Chidthaisong, 2000; Jäckel and Schnell, 2000; Liu et al., 2011; Qu et al., 2004; Teh et al., 2007; Yamada et al., 2014). Also, the capability of these soils for anaerobic methane oxidation (AOM) is currently unknown. We collected topsoils from four Dutch agricultural fields that are drained peatlands and investigated the mobilization of nutrients in the porewater upon artificial inundation. After mimicking inundation for 18 months by adding a water layer, the soil microbial community and its activity were studied by subsequent soil incubations of soil with different electron acceptors during an eight month time period. The microbial succession was assessed by 16S rRNA gene amplicon sequencing for Bacteria and Archaea. The results will be discussed with respect to biogeochemistry, microbial activity and community composition.

2. Materials and methods

2.1. Site description and sampling

Soil cores were collected in March 2016 from four Dutch agricultural fields (three Fe-rich soils named IRS1-3 with increasing number indicating increasing total Fe content and one Fe poor soil named IPS) that are now in use as grasslands (with cattle) situated on top of drained peatlands (so-called peat meadows; Fig. 1, Table 1). They were used as agricultural lands for decades to centuries. None of the fields were located in a nature reserve. Multiple sub-samples from the topsoil layer (0–10 cm below the root zone) were taken at each location with a gouge auger and placed into a glass cylinder (diameter of 14.5 cm). After sample collection, all soils were inundated separately with 1 L of artificial surface water (1.5 M $CaCl_2$, 1 M $MgCl_2$ *6 H_2O, and 2 M $NaHCO_3$), creating a water layer of approximately 10 cm above the soil surface. The inundated soils were placed in a dark climate room with controlled conditions at 15 °C (B-WARE, Nijmegen, Netherlands) to study the mobilization of nutrients over a period of 18 months. Porewater samples (30–40 mL) were taken anoxically using rhizon samplers (Eijkelkamp Agrisearch Equipment) after 1 day (taken as time point 0), 2 weeks, 6 weeks, 12 weeks and 69 weeks of inundation. Samples were analyzed by inductively coupled plasma-optical emission spectrometry (ICP-OES) for Al, Ca, Fe, Mg, Mn, P, and S (iCap 6300, Thermo Scientific, Waltham MA, USA) with a sea spray nebulizer combined with a cyclone chamber. The plasma had a power of 1150 W and was generated by argon gas, with an auxiliary gas flow of 0.5 L min^{-1} and a nebulizer flow of 0.6 L min^{-1}. The porewater samples were also analyzed by continuous flow analysis (CFA) for NO_3, NH_4, PO_4, Na, K, and Cl (Bran + Luebbe Auto Analyzer, SPX Flow, Norderstedt, Germany; Seal Analytical Auto-Analyzer 3, Seal Analytical, Southampton, UK). Gravimetric water content and bulk density of the soil were determined by drying a fixed volume for 48 h at 70 °C. OM content was estimated by loss on ignition for 4 h at 550 °C. To determine total concentrations of Al, Ca, Mg, Fe, P, S, and N, a homogenized portion of 200 mg dry soil was digested in 5 mL HNO_3 (65%) and 2 mL H_2O_2 (30%) using an Ethos 1 Advanced microwave digestion system (Milestone microwave type mls 1200 mega). Digestates were diluted and stored at 4 °C until elemental analysis by ICP-OES (IRIS Intrepid II XDL, Thermo Scientific, Waltham MA, USA). The pH was measured using an Ag/AgCl2 electrode connected to a radiometer (Copenhagen, type TIM840). Alkalinity of surface waters was determined by titration with 0.01 mol L^{-1} HCl until pH 4.2 and concentrations dissolved inorganic carbon (CO_2 and HCO_3^-) in surface and pore water were determined using an infrared gas analyzer (ABB Advance Optima IRGA). Electric conductivity (EC) was measured using an EC-probe (HACH) connected to an HQD-meter.

2.2. Batch incubation experiments

The batch incubation experiments were started in November 2017. For each of the four locations, the water layer on top of the soil was removed and the soil was sieved through a metal sieve (0.42 mm pore size) to remove the remnants of the plant material. Soil slurries were prepared by mixing the soil in a 1:4 weight/volume ratio with anoxic freshwater mineral medium (DSMZ 503) composed of KH_2PO_2 (0.20 g L^{-1}), NH_4Cl (0.25 g L^{-1}), NaCl (1.00 g L^{-1}), $MgCl_2{\cdot}6H_2O$ (0.40 g L^{-1}), KCl (0.50 g L^{-1}) and $CaCl_2{\cdot}2H_2O$ (0.15 g L^{-1}) in grade 3 demineralized water; 1 mL L^{-1} trace element solution SL-10 (DSMZ), with $CeCl_3 \cdot 7H_2O$ 24 mg L^{-1}, $Na_2SeO_3 \cdot 5H_2O$ 30 mg L^{-1} and $Na_2WO_4 \cdot 2H_2O$ 40 mg L^{-1}; and 1 mL L^{-1} of vitamin solution (DSMZ 141). The pH of the slurries was measured (Hanna Instruments, Betuwehaven, the Netherlands) and was between 6.3 and 6.6. Homogenized soil slurry samples of 2.5 mL were taken from all four soils (T0), centrifuged for 10 min at 10,000×*g* (Eppendorf, Nijmegen, The Netherlands) and pellets were stored at −18 °C for subsequent DNA extraction. Activity assays were performed in duplicate in 120 mL glass serum bottles with 53 mL of soil slurry and an end volume of 60 mL after the addition of substrates and/or grade 3 demineralized water. The incubation bottles were sealed with airtight red butyl rubber stoppers and secured with open-top aluminium crimp caps.

2.2.1. Aerobic methanotrophic incubations

For the aerobic methanotrophic incubations 20% CH_4 v/v (final concentration) was added to the oxic headspace filled with air. When the CH_4 concentration was lower than 4 μmol CH_4 mL^{-1} slurry or O_2 was depleted, the headspace of the bottles was three times flushed with 0.2 μM filter-sterilized air before 20% CH_4 v/v, or 21% O_2 v/v was added again, respectively. The serum bottles were incubated by continuous shaking at 100 rpm in the dark for 120 days (platform shaker innova2300, New Brunswick Scientific Europe, The Netherlands). Homogenized soil slurry samples of 2.5 mL were taken aseptically from all incubations after 120 days (T1), centrifuged for 10 min at 10,000×*g* (Eppendorf, Nijmegen, The Netherlands) and pellets were stored at −18 °C for subsequent DNA extraction.

2.2.2. Anaerobic methanotrophic incubations

Anoxic conditions were created in the incubation bottles by three cycles of 15 min vacuuming and 3 min gassing with Argon (Ar). A final overpressure of 0.5 bar was applied in all bottles. Subsequently, 5% CO_2 v/v was added to the headspace. All treatments were performed in duplicates. We used SO_4^{2-} to mimic the actual or geological marine or estuarine settings, N oxides as a result of intense N fertilization, and Fe (III) oxides which naturally accumulate in highly degraded peat soils with Fe-rich topsoil. Following treatments with respective starting concentrations were prepared for each soil: SO_4^{2-} (2 mM), NO_2^- (0.25 mM), NO_3^- (2 mM), ferrihydrite ($Fe(OH)_3$, 10 mM)' and goethite (FeOOH, 10 mM). Each treatment was prepared with and without added ^{13}C-CH_4 (20% v/v final concentration). Control batch incubations of soil slurry were prepared with and without the addition of ^{13}C-CH_4 (20% v/v

final concentration) (Supplemental Table S1).

Ferrihydrite was synthesized by dissolving 35 g of ferric citrate in 300 mL distilled water (80 °C) under vigorous stirring (adapted from Leibl et al., 1999). After cooling to room temperature, the pH was adjusted to 8.0 by the dropwise addition of 10 M sodium hydroxide solution and stirring was continued for 30 min. The resulting ferrihydrite particle suspension was centrifuged at 10,000×*g* at 4 °C for 60 min, the supernatant was discarded and the pellet was resuspended in distilled water. After five cycles of centrifugation, removing the supernatant and resuspension in distilled water, the pellet was resuspended in a small volume of distilled water. Ferrihydrite concentration was determined by measuring the dry weight of an aliquot. Goethite was prepared from an alkaline Fe(III) system according to the protocol by Böhm (1925) as described in Schwertmann and Cornell (1991) with a 72 h incubation at 70 °C.

The serum bottles were incubated horizontally by continuous shaking at 100 rpm in the dark for 240 days (platform shaker innova2300, New Brunswick Scientific Europe, The Netherlands). Liquid samples (0.4mL) were taken during the experiment from the NO_2^-, NO_3^-, and SO_4^{2-} treatments with a syringe. The samples were centrifuged for 10 min at 10,000×*g* (Eppendorf, Nijmegen, The Netherlands) and the supernatant was collected and stored at −18 °C until further processing. All electron acceptors, except Fe(III) oxides, were regularly re-added when necessary from anoxic stock solutions. As one bottle with slurry from IRS2 amended with SO_4^{2-} and CH_4 broke during the experiment, we have a single incubation for this amendment. Homogenized soil slurry samples of 2.5 mL were taken aseptically from all incubations after 120 days (T1) and 240 days (T2), centrifuged at room temperature for 10 min at 10,000×*g* (Eppendorf, Nijmegen, The Netherlands) and pellets were stored at −18 °C for subsequent DNA extraction. The pH of all incubations was measured after 120 and 240 days (Supplemental Table S2).

2.2.3. Denitrification potential

To study the denitrification potential of soil slurries, we added around 2 mM ^{15}N-$NaNO_2$ to NO_2^- amended incubations at a point when non-labeled NO_2^- was depleted (<4.3 μM, using Merckoquant test strips, Merck, Germany). NO_2^- which is the first intermediate of NO_3^- reduction under anoxic conditions can be converted to N_2O, N_2 or ammonium (NH_4^+) as an end product. The ^{15}N label was followed over time by gas measurements and by colorimetric assay for NO_2^- and expressed as rates of N-atom conversion from NO_2^-. The use of ^{15}N-$NaNO_2$ in the incubations enabled the distinction between $^{14/14}N$-N_2 (produced earlier in the experiment) and $^{15/14}N$-N_2 and $^{15/15}N$-N_2 produced from the ^{15}N-$NaNO_2$, as well as the distinction between $^{14/14}N$-N_2O, $^{15/14}N$-N_2O, and $^{15/15}N$-N_2O. ^{15}N-$NaNO_2$ was amended to all bottles except for IRS3 and IPS where one bottle amended with CH_4 and NO_2^- was not depleted yet in NO_2^-. From IRS1, one of the bottles amended with only NO_2^- was excluded from analysis, as it was amended with 1 mM ^{15}N-$NaNO_2$.

2.3. Analytical methods

2.3.1. Gas measurements

Gas samples (50 μL) were taken with a glass syringe (Hamilton, Reno NE, USA). CH_4 was quantified by triplicate injections to an HP 5890 gas chromatograph (Hewlett Packard, Palo Alto CA, USA) equipped with a Porapak Q 100/120 mesh column (Sigma Aldrich, Saint Louis MI, USA) and a flame ionization detector (FID). The quantification of CO_2, O_2, and gaseous N compounds was performed by duplicate injections to a gas chromatograph (6890 series; Agilent, United States) using a Porapak Q column at 80 °C with helium as the carrier gas (flow rate, 24 mL min^{-1}) that was coupled to a mass spectrometer (Agilent 5975C inert MSD; Agilent, United States). Quantification was performed based on calibration curves which were calculated from different volume injections of a standard gas (Linde Gas Benelux BV, The Netherlands). Gas concentration in liquids was calculated using the Ostwald coefficient (Wilhelm et al., 1977). For better comparison of activities and concentrations between the different soils, activities and concentrations are expressed per mL of soil slurry.

2.3.2. NO_2^- and NO_3^- concentration measurements

During the course of incubation experiments, concentrations of NO_2^- and NO_3^- were first estimated using Merckoquant Nitrate test strips (0–113 mg L^{-1}; Merck, Germany). Aliquots (0.4 mL) were taken and stored at −18 °C until analysis. Concentrations of both NO_2^- and NO_3^- were measured in triplicate using the Griess assay (Griess-Romijn van Eck, 1996) on the microplate spectrophotometer (Spectramax 190, Molecular Devices, The Netherlands). For the determination of NO_3^- concentration an additional step was performed: vanadium(III) was added to reduce NO_3^- to NO_2^-, and the concentration of NO_2^- was subtracted from the total NO_2^- measured (Miranda et al., 2001).

2.3.3. SO_4^{2-} determination

Aliquots of liquid samples (0.4 mL) were diluted 20 to 50 times with 0.1% nitric acid to a final volume of 4 mL. The SO_4^{2-} concentration was determined by measuring the total S concentration in the sample by ICP-OES (iCap 6300, Thermo Scientific, Bremen, Germany) with a sea spray nebulizer combined with a cyclone chamber. The plasma had a power of 1150 W and was generated by argon gas, with an auxiliary gas flow of 0.5 L min^{-1} and a nebulizer flow of 0.6 L min^{-1}.

2.4. Molecular analysis

2.4.1. DNA extraction

DNA was extracted with the PowerSoil DNA Isolation Kit (MO BIO, Qiagen, Venlo, the Netherlands) following the manufacturer's instructions with the modification of adding a 3 min bead beating step (Mixer Mill MM 400, Retsch GmbH, Germany) at 30 bps instead of PowerBead Tube vortexing step. Quantity and quality of the DNA were measured by the NanoDrop 1000 (Invitrogen, Thermo Fisher, Carlsbad CA, USA) and the Qubit spectrophotometer using the dsDNA HS Assay Kit (Invitrogen, Thermo Fisher, Carlsbad CA, USA) according to the manufacturer's instructions. Extracted DNA from duplicate incubations was pooled in equimolar concentration. DNA was stored at −18 °C until further processing.

2.4.2. Phylogenetic analysis

The community composition and diversity of Bacteria and Archaea were assessed by the 16S rRNA gene amplicon sequencing. Sequencing was performed on an Illumina Miseq Next Generation Sequencer by Macrogen, Korea. Primers used for amplification were Bac341F (5′-CCTACGGGNGGCWGCAG-3′) (Herlemann et al., 2011) and Bac806R (5′- GGACTACHVGGGTWTCTAAT-3′) (Caporaso et al., 2012) for Bacteria and Arch349F (5′-GYGCASCAGKCGMGAAW-3′) and Arch806R (5′-GGACTACVSGGGTATCTAAT-3′) (Takai and Horikoshi, 2000) for Archaea. A two-step PCR was performed with 12.5 ng of genomic DNA (2.5 μL), 5 μL of forward and reverse primer (1 μM), and 12.5 μL of 2x KAPA Hifi Hotstart ready mix using the following thermal program: 3 min at 95 °C, 30 s at 95 °C, 30 s at 55 °C, and 30 s at 72 °C (these last three steps were repeated for 25 cycles), finished by 5 min at 72 °C. PCR products were purified using AMPure XP beads. The purified PCR products (5 μL) were used for the second PCR (same PCR protocol with only 8 cycles) in combination with sample-specific barcoded primers (Nextera XT index kit, Illumina). The produced PCR library was cleaned by AMPure XP beads and quantified by using the Bioanalyzer DNA 1000 chip. Subsequently the libraries were sequenced on an Illumina MiSeq with 2 × 300bp chemistry. The number of reads generated is stated in Supplemental Tables S3 and S4.

The first steps of data analysis were conducted in CLC Genomics Workbench v. 11 (QIAGEN Aarhus A/S, Denmark) by removing the primers by trimming the first 20 nucleotides of all sequences. Further processing was performed with the DADA2 Pipeline (1.8) (Callahan

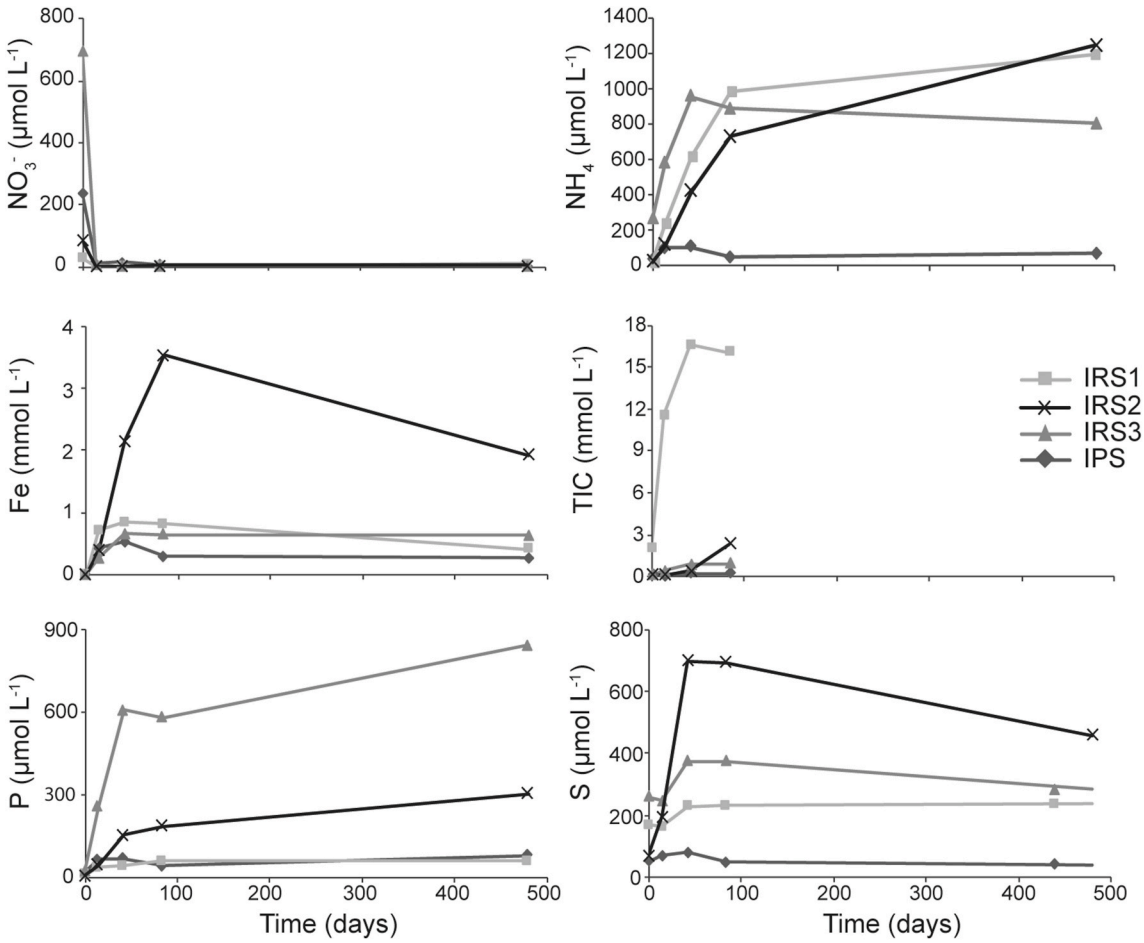

Fig. 2. Mobilization of nitrate (NO_3^-), ammonium (NH_4^+), iron (Fe), total inorganic carbon (TIC), phosphorus (P), and sulfur (S) over time (t = 0, 2, 6, 12, 69 weeks) in the porewater of the four experimentally inundated agricultural drained peat soils (pre-batch incubation period). The concentration of TIC was only measured till week 12.

et al., 2016) following the standard operating procedure in Rstudio (RStudio Team, 2015). Reads were quality filtered (default settings) and trimmed to 280 base pairs for the forward read and to 220 base pairs for the reverse reads. Subsequently, the error rates in the sequences were learned and the DADA2 algorithm was applied. Reads were merged, chimeras were removed, and taxonomy was assigned. Taxonomic classification was performed by using the SILVA v132 16S rRNA gene non-redundant database (SSURef_NR99_132_SILVA) as a reference. Reads identified as 'Bacteria' and 'Archaea' were selected for the bacterial and archaeal sequence datasets, respectively, and 'Mitochondria' were removed from the bacterial sequence datasets ('Chloroplasts' were not detected). The number of sequences after each step of processing can be found in Supplemental Tables S3 and S4. Archaeal reads were rarefied on 720 reads (discarding sequences from IRS1 sample with NO_2^- and CH_4 from the time point of 240 days with 420 sequences) and bacterial reads on 2560 reads (Supplemental Fig. S1). Data was visualized using R packages phyloseq (McMurdie and Holmes, 2013), ggplot2 (Wickham, 2016) and vegan (Oksanen et al., 2018). All sequencing data was submitted to the GenBank databases under the BioProject with accession number PRJNA562618.

3. Results

We studied the effect of inundating in four peat topsoils (Fig. 1) with respect to porewater quality, microbial activity and community composition upon different substrate amendments, and potential GHG fluxes. The soils varied in OM content, texture, and total Fe concentration (Table 1).

3.1. Changes in nutrient release in relation to porewater biogeochemistry upon inundation

The four topsoils were artificially inundated for 18 months, which led to profound changes in the porewater chemistry. These changes were related to the soil type and affected the initial availability of the substrates present (Supplemental Tables S3 and S4). Experimental inundation resulted in a rapid decrease of NO_3^- concentration within two weeks in all soils. Concentrations of porewater Fe, total inorganic carbon (TIC), NH_4^+, and P increased in all incubations in response to water saturation. The magnitude of this effect was the strongest in the Fe-rich soils IRS1, IRS2, and IRS3 (Fig. 2). The NH_4^+ concentration increased up to approximately 1 mmol L^{-1} in all three Fe-rich soils while it remained an order of magnitude lower (maximum 0.1 mmol L^{-1}) in the IPS (Fig. 2). Total dissolved P reached the highest concentration in IRS3, which had the highest total Fe concentration, followed by the IRS2 (Fig. 2).

3.2. Methanogenic activity

The effect of electron acceptor availability (NO_3^-, NO_2^-, SO_4^{2-}, Fe(III) mineral forms ferrihydrite and goethite) on the CH_4 dynamics in the different soils was investigated in batch incubations (Fig. 3, Table 2). In the presence of both Fe(III) oxide forms the net methanogenic activity was neither significantly suppressed nor enhanced in any of the soil

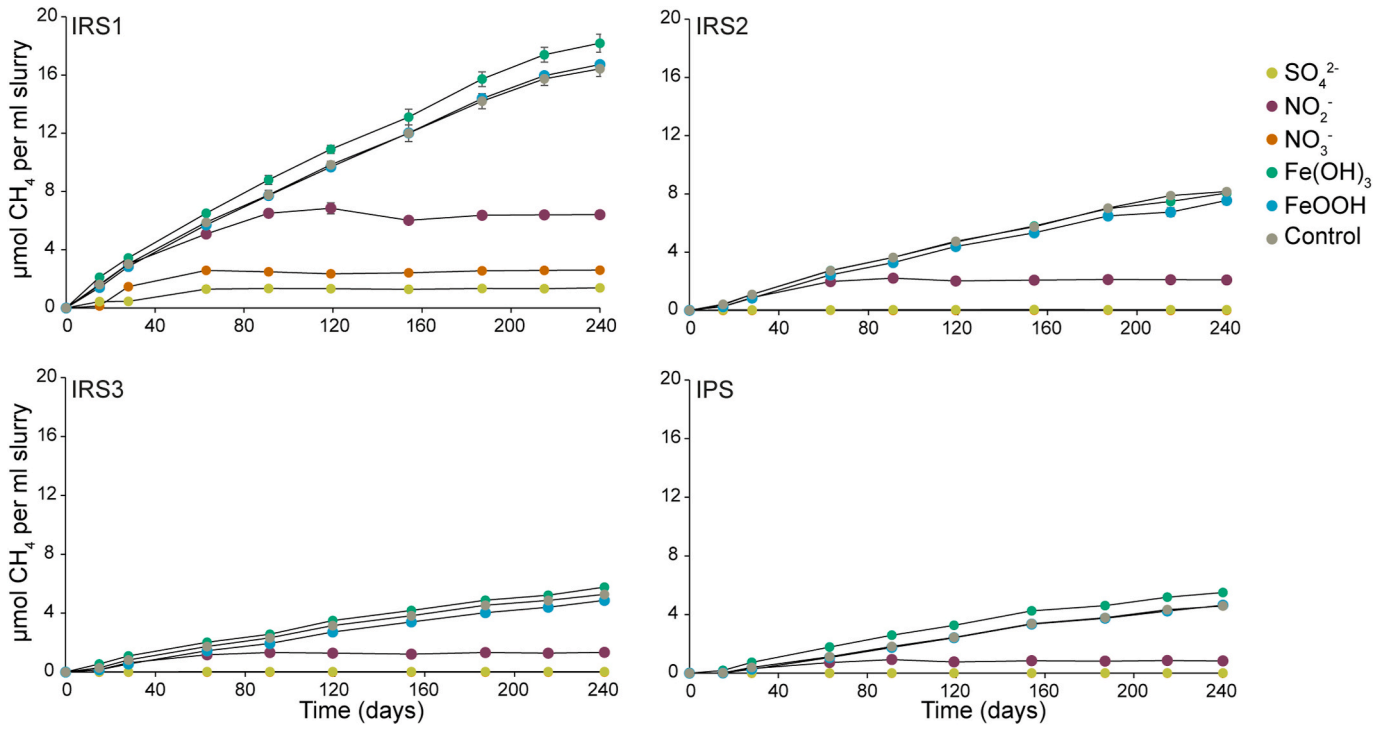

Fig. 3. Methane (CH_4) production rates in batch incubations for the four investigated soils amended with nitrite (NO_2^-), nitrate (NO_3^-), sulfate (SO_4^{2-}), ferrihydrite ($Fe(OH)_3$), goethite (FeOOH), and the control without added electron acceptors. The graphs show the average of duplicate batch incubation.

Table 2
Maximum methane (CH_4) production rates in nmol CH_4 mL^{-1} slurry day^{-1} in batch incubations amended with sulfate (SO_4^{2-}), nitrite (NO_2^-), nitrate (NO_3^-), ferrihydrite ($Fe(OH)_3$), goethite (FeOOH), and in the control without electron acceptor additions. Maximum CH_4 production rates were calculated after 100 days of incubation.

Soil	SO_4^{2-}	NO_2^-	NO_3^-	Fe $(OH)_3$	FeOOH	Control
IRS1	1.3 (±0.2)	8.3 (±0.3)	2.9 (±0.6)	59 (±8.2)	65 (±3.8)	59 (±11)
IRS2	0.5 (±0.0)	0.5 (±0.7)	0.06 (±0.1)	37 (±1.9)	30 (±6.1)	32 (±4.6)
IRS3	0.03 (±0.004)	2.8 (±0.4)	0.009 (±0.005)	20 (±2.5)	16 (±1.6)	15 (±0.6)
IPS	0.03 (±0.04)	1.1 (±0.7)	0.006 (±0.002)	23 (±0.2)	23 (±0.02)	22 (±1.6)

slurry incubations in comparison to control incubations. The presence of NO_3^-, NO_2^-, and SO_4^{2-} inhibited the methanogenic activity. NO_3^- and NO_2^- were provided regularly during the experiment to avoid exhaustion due to the high denitrification rates in the soils (Supplemental Figure S2, S3 and S4). However, time periods with lower concentrations or depletion of these substrates, especially during the first 100 days of the experiment for NO_2^-, still occurred, resulting in temporal CH_4 production (Fig. 3).

3.3. Methanotrophic activity

The CH_4 produced by the methanogens can be oxidized by both aerobic and anaerobic methanotrophs when suitable electron acceptors are sufficiently present. The potential for AOM was assessed by the conversion of ^{13}C-CH_4 into ^{13}C-CO_2 (Supplemental Fig. S5). The production of ^{13}C-CO_2 was only detected in the incubations amended with Fe(III) oxides and controls without added electron acceptors. The ^{13}C-CO_2 production followed the same trend as the CH_4 production, and the presence of NO_2^-, NO_3^- and SO_4^{2-} inhibited both ^{13}C-CO_2 production and methanogenesis. The concentration of ^{13}C-CO_2 in the headspace did not exceed 0.08 µmol per mL slurry and formed up less than 0.9% of the total cumulative ^{13}C-CH_4 amended into the bottles. Aerobic methanotrophy became active in all soils after a lag phase of around 30 days from the time the slurries were exposed to O_2. Their activity was similar for all soils oxidizing ~196 µmol CH_4 mL^{-1} slurry in 120 days (Table 3).

Table 3
Maximum methane (CH_4) oxidation rates and total CH_4 consumed in 120 days. Units in µmol CH_4 mL^{-1} slurry.

Soil	Max CH_4 oxidation	Total CH_4 oxidized
IRS1	4.2 (±0.1)	192 (±1.8)
IRS2	4.7 (±0.1)	189 (±6.8)
IRS3	3.6 (±0.01)	208 (±1.1)
IPS	3.5 (±0.01)	194 (±0.6)

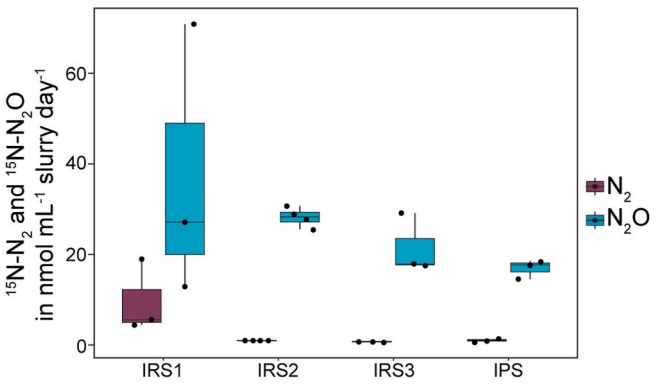

Fig. 4. Rates of ^{15}N-N_2 and ^{15}N-N_2O production in the batch incubations amended with ^{15}N-NO_2 in the four investigated soils.

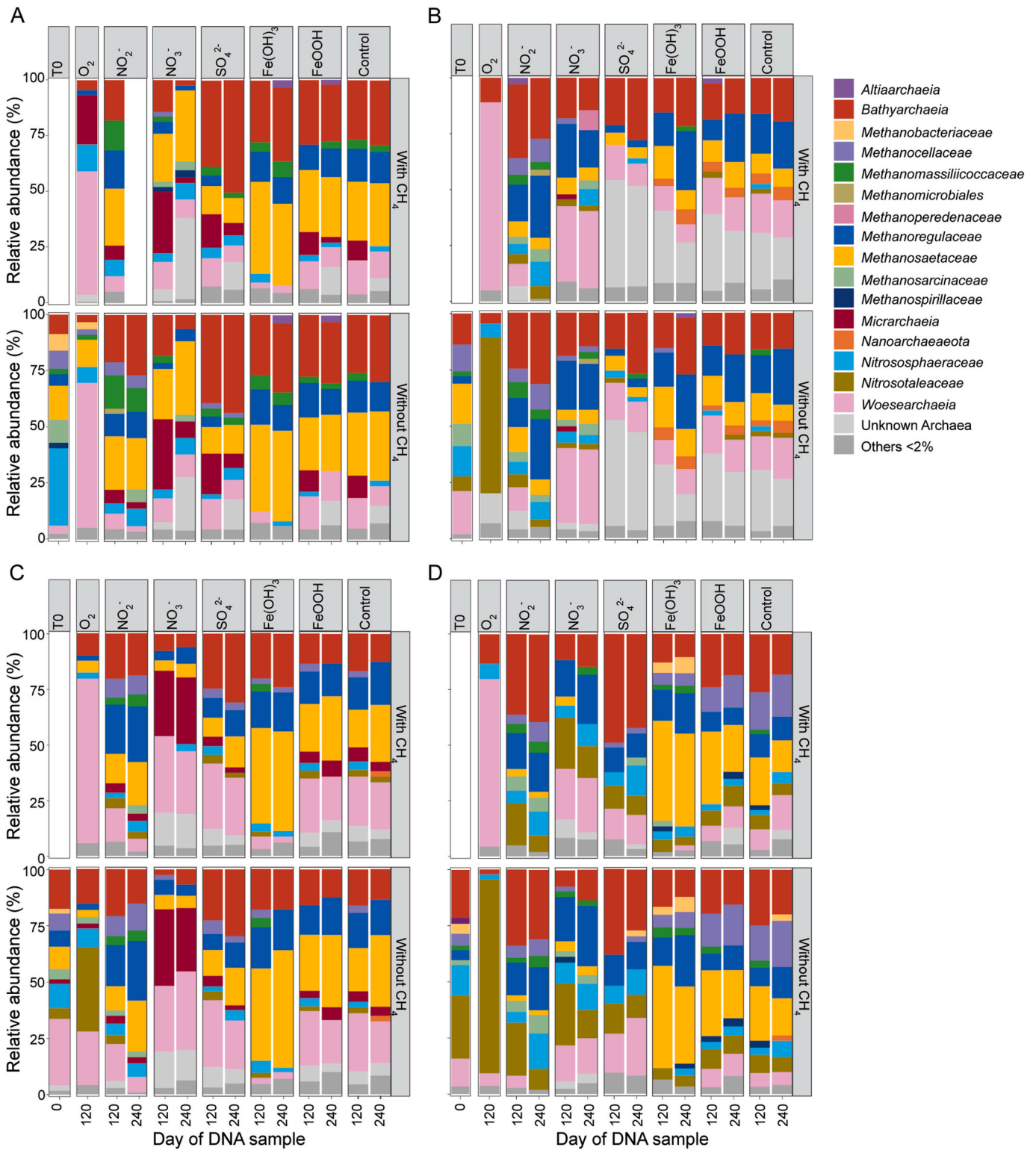

Fig. 5. Taxonomic distribution of archaeal 16S rRNA gene amplicon sequences on family level for the four investigated soils a) IRS1, b) IRS2, c) IRS3, and d) IPS at three time points of the batch incubation experiment (days 0, 120, 240) with and without additions of substrates.

3.4. Denitrification potential

The reduction of NO_2^- and NO_3^- occurred in all slurries and the rates differed per soil. Highest rates were detected in the IRS1 and IRS2 (172 ± 60 and 191 ± 17 nmol NO_2^- mL^{-1} slurry day^{-1}, and 136 ± 11 and 49 ± 7 nmol NO_3^- mL^{-1} slurry day^{-1} respectively), whereas the rates in IRS3 and IPS were nearly 3 times lower (53 ± 4 and 52 ± 4 nmol NO_2^- mL^{-1} slurry day^{-1}, and 35 ± 2 and 25 ± 5 nmol NO_3^- mL^{-1} slurry day^{-1} respectively). To quantify the denitrification products, the incubations that previously received NO_2^- were amended with ^{15}N-NO_2^- (~2 mM) after the unlabeled pool of NO_2^- was exhausted. N_2O was detected in all soils (Fig. 4). In IRS1 and IRS2, only 20% and 10% respectively of the ^{15}N label from ^{15}N-NO_2 could be recovered in N_2O ($^{14/15}N_2O$ and $^{15/15}N_2O$ respectively) in a period between 30 h and 126 h after the

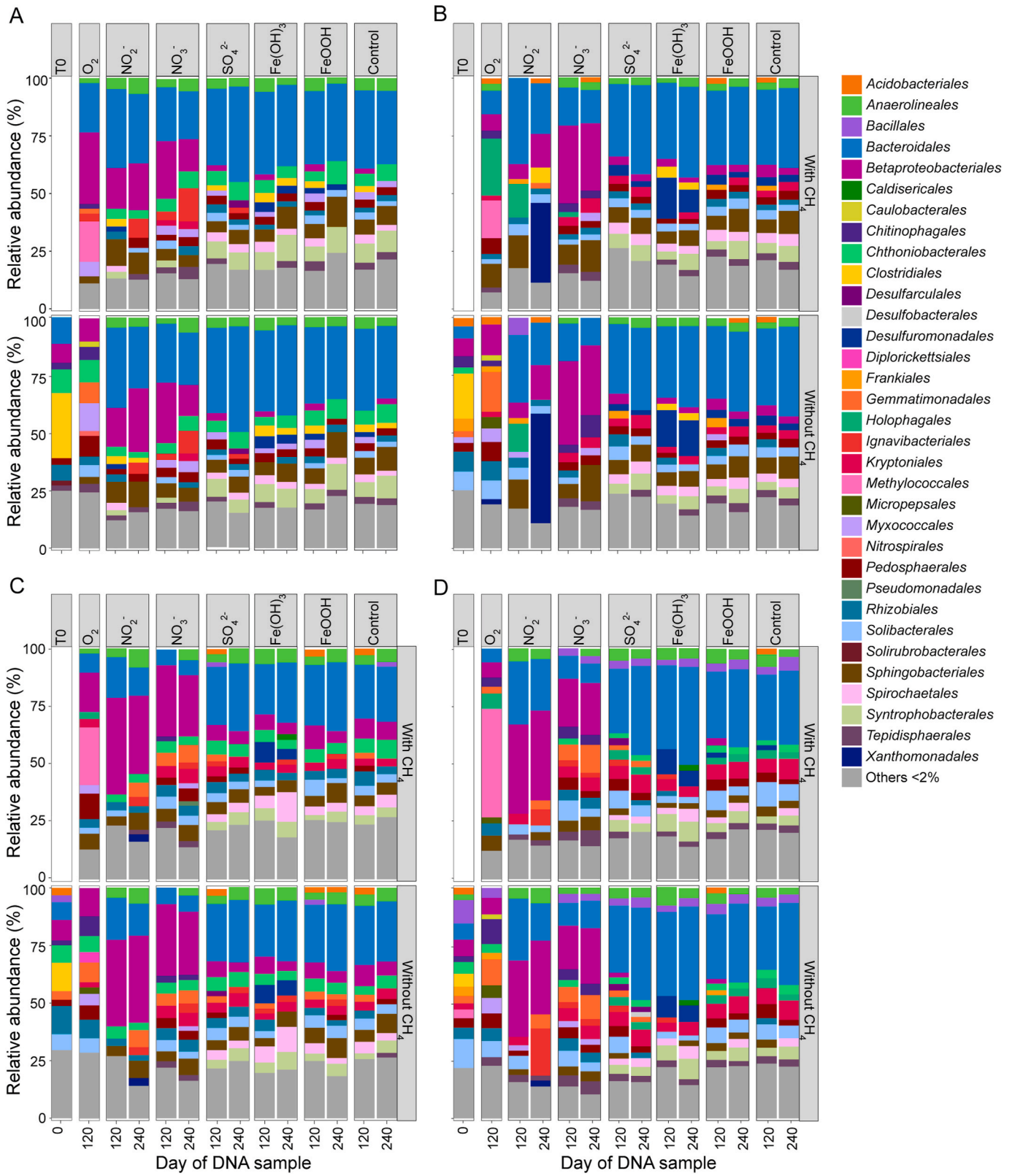

Fig. 6. Taxonomic distribution of bacterial 16S rRNA gene amplicon sequences on order level for the four investigated soils a) IRS1, b) IRS2, c) IRS3, and d) IPS at three time points of the batch incubation experiment (days 0, 120, 240) with and without additions of substrates.

addition of $^{15}N\text{-}NO_2^-$. For IRS3 and IPS, both exhibited lower NO_2^- reduction rates, the recovery of the ^{15}N label in N_2O was 40% and 20% of the consumed $^{15}N\text{-}NO_2^-$ respectively. The evolution of N_2 ($^{14/15}N_2$ and $^{15/15}N_2$) was only observed in IRS1 (between 4.4 and 19 nmol N_2 mL^{-1} slurry day^{-1}).

3.5. Changes in the archaeal community composition

Biomarkers of putative methanogenic archaea showed the highest relative abundance in the incubations amended with Fe(III) oxides and controls without additions (Fig. 5), coinciding with the observed CH_4 production rates (Fig. 3). The methanogenic taxa consisted of *Methanoregulaceae* and *Methanosaetaceae* (recently reclassified as *Methanotrichaceae* (Parks et al., 2017)). *Methanoregulaceae* dominated in the IRS2 at both Fe(III) oxide amended and control incubations (relative archaeal abundance to 9% and 26%), while *Methanosaetaceae* were more abundant in the soil prior to batch incubations (relative abundance of 18%) and decreased in relative abundance during the incubations (to 7%–18%). In the IRS1, IRS3, and IPS, *Methanosaetaceae* were the most abundant methanogens (relative archaeal abundance of 17%–46%), which was in line with their presence in the soils of IRS1 and IRS3 prior to the batch incubations (15% and 10% relative abundance respectively). This family was not detected in the IPS prior to the batch incubations. Here, *Methanocellaceae* was the most abundant methanogenic family (relative abundance of 5%). *Methanocellaceae* increased in relative abundance in incubations with goethite and the controls (after 120 days relative abundance of 11%–15%, after 240 days 15%–21%). IPS had the most diverse methanogenic community at the end of the incubations. In all incubations, *Methanosarcinaceae* methanogens became outcompeted despite the initial presence in all soils (relative abundance of 2%–10%).

The known anaerobic CH_4 oxidizers classified as '*Candidatus* Methanoperedens nitroreducens' were only detected in the NO_3^- and ^{13}C-CH_4 amended incubations after 240 days in IRS2, reaching a relative abundance of 9% of total archaeal reads (Fig. 5). Despite of their enrichment in the IRS2, no AOM activity could be detected in these incubations. Neither NO_2^- nor SO_4^{2-} dependent AOM microorganisms known, could be detected in the 16S rRNA gene amplicon data.

3.6. Changes in the bacterial community composition

The bacterial community structure changed over the course of incubation with the different substrates (Fig. 6). In incubations amended with NO_2^- and NO_3^-, *Betaproteobacteria* became the most dominant class of Bacteria after both 120 and 240 days of incubation (Fig. 6). The detected betaproteobacteria were dominated by the families *Burkholderiaceae* and *Hydrogenophilaceae* at all sampling points (Supplemental Fig. S6). *Rhodanobacteriaceae* family dominated the bacterial community in NO_2^- incubations of IRS2 after 240 days (relative abundance of 35% and 47% without and with CH_4 addition, respectively, Supplemental Fig. S6), while it was under the detection limit at the other time points. An enrichment of *Gallionelaceae* was detected in IRS1, IRS3, and IPS in incubations amended with both NO_2^- and NO_3^- and in IRS2 only in NO_3^- amended incubations after both 120 and 240 days of incubation (relative abundance between 2% and 27%) (Supplemental Table S7). Also, the presence of ferrihydrite triggered changes in bacterial community composition in comparison to goethite amended and control incubations, which remained more similar to one another (Supplemental Fig. S6). The amendment of ferrihydrite triggered the enrichment of *Geobacteraceae* (relative bacterial abundance between 3% and 18%) in all soil slurries (Supplemental Table S7). *Geobacteraceae* sequences were below the detection limit prior to incubation.

The most abundant aerobic methanotrophs detected in all oxic incubations belonged to the *Methylococcales* with *Methylomonaceae* as the dominant family (Fig. 6, Supplemental Table S7). It reached the highest relative abundance in IPS (47% of the bacterial reads) and lowest in soil IRS2 (16%), showing that the abundance in the soils did not correlate with the detectable activity (Table 3). In addition to *Methylomonaceae*, the IRS3 incubations also showed a relative enrichment in *Methylococcaceae* after 120 days (2% of total bacterial amplicon sequence variants (ASVs), Supplemental Table S7). This group of methanotrophs was below the detection limit in the soils prior to batch incubations. Sequences belonging to *Methylophilaceae* family were detected in all the batch incubations with relative abundance above 2% (Supplemental Table S7).

4. Discussion

This study investigated the effects of the addition of different electron acceptors mimicking diverse conditions, on the activity and composition of the microbial community of Fe-rich drained peatlands subject to inundation as land restoration management strategy. Topsoil samples were collected from four different locations in the Netherlands, with a gradient in total Fe concentrations (low-rich-very rich).

4.1. Effect of inundation and Fe concentrations on carbon and nutrient biogeochemistry

Inundation was simulated for 1.5 years in the laboratory by the use of artificial freshwater resulting in increased concentrations of Fe, NH_4^+, and P in the porewater. Similar results were reported by other studies (Emsens et al., 2016; Harpenslager et al., 2015; Zak et al., 2018). The observed accumulation of NH_4^+ as well as total dissolved Fe and TIC in all Fe-rich soils can be explained by higher rates of Fe-mediated anaerobic degradation of OM, which triggers the conversion of organic-N to inorganic-N and releases NH_4^+. The high concentrations of TIC in the Fe-rich soils were mainly related to anaerobic reduction processes coupled to OM decomposition, in combination with lower CO_2 diffusion rates as a result of flooding. The high concentration of dissolved P in IRS2 could be related to higher S loads at this site, since SO_4^{2-}, and particularly sulfide produced by microbial reduction, can enhance internal eutrophication (Lamers et al., 2002; Smolders et al., 2006). This change in porewater quality will affect ecosystem functioning and could very well lead to eutrophication.

4.2. Ferric iron does not suppress methanogenesis in inundated peat soils

To investigate how the microbial community in inundated soils would respond to the exposure of ecosystem-relevant oxidants such as NO_2^-, NO_3^-, SO_4^{2-} and Fe(III) oxides, activity measurements and the succession of microbial communities were investigated. Interestingly, neither forms of Fe(III) oxide (ferrihydrite and goethite) applied suppressed methanogenesis in inundated peat soils. These Fe(III) oxides are abundant in soils, but differ greatly in their crystallinity and bioavailability for microbial Fe(III) reduction, with ferrihydrite being the thermodynamically most favorable Fe(III) oxide (Childs, 1992; Cornell and Schwertmann, 2003; Lovley et al., 1991; Lovley and Phillips, 1986; Phillips et al., 1993). The effect of Fe(III) oxide supplementation on methanogenesis in soils has been studied previously. In several studies an inhibitory effect on methanogenesis was observed, which was explained by unfavorable thermodynamics or substrate competition in the presence of heterotrophic Fe(III) oxide reduction (Bodegom et al., 2004; Chidthaisong, 2000; Jäckel and Schnell, 2000; Liu et al., 2011; Qu et al., 2004; Teh et al., 2007; Yamada et al., 2014). However, recent studies have reported stimulation of CH_4 production by (semi)conductive Fe(III) oxides (Cruz Viggi et al., 2014; Kato et al., 2012; Kato and Igarashi, 2019; Li et al., 2015; Tang et al., 2016; Zhou et al., 2014; Zhuang et al., 2015). Here, we did not observe a detectable effect on methanogenic activity.

4.3. Higher relative abundance of methanogens and Fe(III)-reducing bacteria induced by ferrihydrite

The ferrihydrite addition led to the higher relative abundances of methanogens and Fe(III) reducing Bacteria. The methanogenic taxa consisted mainly of *Methanoregulaceae* (mostly hydrogenotrophic methanogens (Brauer et al., 2011)) and *Methanosaetaceae* (mostly acetoclastic methanogens (Jetten et al., 1992)). Abundant *Methanosaetaceae*

were also previously observed in rewetted fens that were characterized by high CH_4 emissions (Wen et al., 2018). A recent study has shown that acetoclastic methanogens can also reduce Fe(III) with acetate for respiratory growth (Prakash et al., 2019). This could be one of the possible reasons why acetoclastic *Methanosaetaceae* increased in relative abundance in ferrihydrite amended incubations without higher CH_4 production rates compared to controls. *Geobacteraceae* biomarkers were only detected in the ferrihydrite amended batch incubations. *Geobacteraceae* bacteria are abundant in soils where they employ dissimilatory Fe(III) reduction with various organic substrates (Caccavo et al., 1994; Lovley et al., 2004, 1993). Our results show that the community composition of Fe(III) reducing bacteria depended on Fe(III) oxide mineralogy and availability. The enrichment of *Geobacteraceae* with additional ferrihydrite could also lead to syntrophic associations with *Methanosaetaceae* methanogens when acetate becomes scarce and magnetite accumulates upon reduction of ferrihydrite (Rotaru et al., 2014). Both organisms can cooperate via direct electron transfer where *Methanosaeta* scavenges the electrons from *Geobacter* and acts as an electron acceptor (Rotaru et al., 2014). During this syntrophic metabolism, *Methanosaeta* methanogens perform CO_2 reduction with electrons derived from *Geobacter* (Rotaru et al., 2014). Other factors such as temperature or pH can also influence the balance between methanogenesis and Fe(III) reduction in a system with Fe(III) oxide minerals was further shown to be dependent on temperature and pH (Aromokeye et al., 2018; Marquart et al., 2019).

4.4. Long-term exposure to nitrogen oxides suppresses methanogenesis but leads to the production of N_2O

Exposure of soil slurries to NO_2^-, NO_3^-, and SO_4^{2-} inhibited methanogenesis corroborating previous studies (Klüber and Conrad, 1998a, 1998b; Lovley et al., 1982; Roy and Conrad, 1999; Scholten and Stams, 1995). The long-term exposure to N oxides resulted in production of N_2O. The increase in N_2O production upon rewetting has been reported previously and isisi attributed to the increase in the denitrification activity when N oxides were present (Beare et al., 2009; Harrison-Kirk et al., 2013; Liu et al., 2018; Ruser et al., 2006; Snider et al., 2015). The nitrite reduction rates found (to 0.06–0.21 μmol N g^{-1} dry weight h^{-1}) were in the range of the rates found in studies with comparable experimental set ups, ranging from 0.007 μmol N g^{-1} dry weight h^{-1} in clay loam soil to 0.6 μmol N g^{-1} dry weight h^{-1} in an arable field (Enwall et al., 2005; Holtan-Hartwig et al., 2000; Van Den Heuvel et al., 2011). Nonetheless, this resulted in lower N_2:N_2O ratio compared to previous studies (Holtan-Hartwig et al., 2000; Rudaz et al., 1991; Van Den Heuvel et al., 2011). The biological denitrification depends on several factors including C content, pH, inorganic N content, copper availability, soil texture, and microbial community (Felgate et al., 2012; Harrison-Kirk et al., 2013; Ruser et al., 2006; Van Den Heuvel et al., 2011, 2010), which could have contributed to the differences in N_2O production rates per soil. The evolution of N_2 ($^{14/15}N_2$ and $^{15/15}N_2$) was only observed in IRS1, which points to differences in the composition and functionality of the microbial community in analyzed soils.

The incubations with added N oxides became dominated by bacterial groups putatively involved in autotrophic N oxide reduction with Fe(II) and S that were already present in the soils, and indicate a significant role of Fe(II) as electron donor compared to organic C. High relative abundance was detected for example for *Burkholderiaceae*, known to perform autotrophic NO_3^- dependent Fe(II) oxidation (Carlson et al., 2013; Kiskira et al., 2017; Straub et al., 2004), and for *Hydrogenophilaceae* which are able to oxidize ferrous sulfide (FeS) and various reduced inorganic S compounds in the presence of NO_3^- (Hedrich et al., 2011; Straub et al., 1996). The studied IRS1-3 were rich in Fe(III) oxides that upon reduction could serve as an electron donor to these putative Fe (II) oxidizers. In addition, the family *Gallionelaceae*, detected in all soils upon N oxide addition except for IRS2 with NO_2^-, comprises many characterized microaerophilic Fe(II) oxidizing bacteria (Ehrenberg, 1836). Previous studies have also provided evidence for their involvement in Fe(II) oxidation with NO_3^- as terminal electron acceptor (Blothe and Roden, 2009; He et al., 2016; Kanaparthi et al., 2013; Nordhoff et al., 2017). This showed that incubations with added N oxides became dominated by bacterial groups putatively involved in autotrophic N oxide reduction with Fe(II) and S, and indicate the dominant role of Fe (II) as electron donor over organic C. Furthermore, the *Rhodanobacteriaceae* family which became highly abundant in IRS2 includes many members capable of complete denitrification (Kostka et al., 2012; Van Den Heuvel et al., 2010). However, no N_2 formation was detected in this soil, which could be the result of electron donor shortage due to exhaustion of labile organic C during inundation, low pH, or limitation of copper (Felgate et al., 2012; Van Den Heuvel et al., 2011, 2010). Besides microbial denitrification, some abiotic chemodenitrification that involves NO_2^- and Fe(II) could also be responsible for some of the N_2O formation at neutral pH (Grabb et al., 2017; Heil et al., 2014; Jones et al., 2015). The increase of N_2O production is an adverse effect of inundation and should be studied in more detail, taking also vegetation into account.

4.5. Potential for anaerobic methanotrophy

The electron acceptors NO_2^-, NO_3^-, and SO_4^{2-} can all potentially be used by anaerobic CH_4 oxidizing Archaea and Bacteria (Boetius et al., 2000; Cai et al., 2018; Haroon et al., 2013; Raghoebarsing et al., 2006). The potential for AOM was assessed by the conversion of ^{13}C-CH_4 to ^{13}C-CO_2. The production of ^{13}C-CO_2 was only detected in the incubations amended with Fe(III) oxides and control incubations without added electron acceptors. The ^{13}C-CO_2 production followed the same trend as the CH_4 production, and the presence of NO_2^-, NO_3^- and SO_4^{2-} inhibited both ^{13}C-CO_2 production and methanogenesis. The concentration of ^{13}C-CO_2 in the headspace did not exceed 0.08 μmol per mL slurry and formed up to 0.9% of the total ^{13}C-CH_4 amended to the bottles. With this small amount of ^{13}C produced we cannot exclude the process of trace CH_4 oxidation (TMO) that has been demonstrated for pure cultures of active methanogens (Timmers et al., 2017). Known anaerobic CH_4 oxidizers classified as '*Candidatus* Methanoperedens nitroreducens' were only detected in the NO_3^- and ^{13}C-CH_4 amended incubations after 240 days in IRS2. These organisms belong to the anaerobic methanotrophic archaea clade 2d (ANME-2d), which are known to perform NO_3^- and Fe(III) dependent AOM in freshwater systems (Cai et al., 2018; Haroon et al., 2013). Similar enrichment timcxsdxxxxxxxxxxxxxe for NO_3^- dependent AOM was reported by Vaksmaa et al. (2017) where significant growth was detected after 9 months of enrichment. Interestingly, despite the onset of ANME-2d enrichment, no AOM activity could be detected in these incubations that could be explained by a requirement of minimum population size for the onset of measurable activity. Neither NO_2^- nor SO_4^{2-} dependent known AOM microorganisms could be detected in the 16S rRNA amplicon data. It is possible that AOM microorganisms need longer time frames for enrichment in inundated peat soils.

4.6. High potential for aerobic methanotrophy under oxic conditions

The potential for aerobic CH_4 oxidation is relevant for agricultural areas where rewetting occurs in short cycles or when the water table is below the soil surface level. The results showed that aerobic methanotrophs quickly become active and enriched in agricultural peat soils when O_2 and CH_4 are supplied. For rewetting practices, optimal conditions to establish a methanotrophic population would include a water table level just below the soil surface. Such conditions may minimize the diffusive fluxes of CH_4 to the atmosphere (Couwenberg, 2009).

5. Conclusions and outlook

Sustainable, climate-smart management strategies are needed to

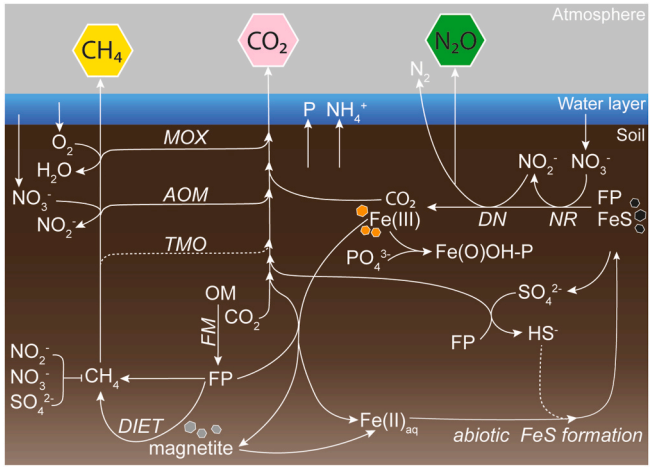

Fig. 7. Schematic overview of the main microbial and chemical processes that are hypothesized to occur in the investigated iron-rich peat topsoils upon rewetting based on the observed activities and microbial community composition. Abbreviations of microbial processes (italics): MOX, aerobic methane oxidation; AOM, anaerobic oxidation of methane; TMO, trace methane oxidation by methanogens; FM, fermentation; DIET, direct electron transfer; DN, denitrification; NR, nitrate reduction. Abbreviations of compounds: OM, organic matter; FP, fermentation products (including organic acids, alcohols, H_2). The time scales for the establishment of individual processes depicted in the figure will differ and depend on the availability of substrates, soil properties and the starting microbial community.

restore drained peatlands that simultaneously would prevent the harmful GHG emissions from these soils. Large-scale rewetting is currently put in practice and planned for the near future to prevent further degradation of peat soils and subsidence, and to lower GHG (mainly CO_2) emissions. Although rewetting is essential for the restoration of drained peatlands, the reduction in GHG emissions after rewetting largely depends on the interactions between the geochemical conditions and the microbial community present in these soils. Permanent inundation of degraded fertilized peatlands with Fe-rich topsoils will lead to increases in methanogenic abundance and potentially activity, subsequently leading to higher CH_4 emissions when inhibitors such as N oxides and SO_4^{2-} become depleted. Unexpectedly, abundant Fe (III) oxide availability did not inhibit methanogenesis. None of the amended electron acceptors stimulated detectable AOM activity during the investigated period of 8 months. However, the onset of ANME-2d enrichment towards the end of the incubation period with added CH_4 and NO_3^- scenario shows that AOM communities may require even longer periods to establish and become significantly active. Moreover, the possible establishment of AOM populations will depend on the initial microbial community of a particular soil and sufficient supply of electron acceptors. Inundation with N-rich water will stimulate denitrification, which may lead to elevated short-term emissions of N_2O depending on prevailing soil geochemical conditions and microbial community. The potential processes that could play a major role upon inundation of Fe-rich peat topsoils are summarized in Fig. 7. Elevated emissions of CH_4 and increased production of N_2O are major adverse effects in the early stages of inundation. In the long run (years to decades), inundation is assumed to have a net GHG sequestration effect. The current strategies are idealistic in restoring exhausted peatlands and thereby combating CO_2 emissions, but may impose elevated emissions of even more potent greenhouse gases CH_4 and N_2O, at least on the short term. In essence, although we are convinced that rewetting is an essential step in order to restore peatland ecosystems functioning and services, the management of these soils needs to apply additional and more site-specific strategies to minimize emissions of CH_4 and N_2O. Applicable inundation strategies of eutrophic Fe(III) oxide-rich peatlands could include the removal of the Fe-rich topsoil to prevent both eutrophication and increase in CH_4 emissions. Additionally, peat soils could be inundated with application of vegetation like *Sphagnum* or *Typha latifolia* species which decreases CH_4 emissions. Maintenance of an elevated water table just below the soil surface level to prevent anoxic conditions in the topsoil could also be used to combat the CH_4 emissions.

Declaration of competing interest

The authors declare that they have no known competing financial interests or personal relationships that could have appeared to influence the work reported in this paper.

Acknowledgments

We would like to thank Sebastian Krosse and Deef van Houdt for pore water measurements, and Martine Kox, Jeroen Frank and Tijs van den Bosch for help with DADA2 implementation. This work was supported by the Netherlands Organization for Scientific Research (NESSC 024.001.001 to M.S.M.J., A.E.E.J., O.R. and SIAM 024.002.001 to M.S.M.J.) and the European Research Council (ERC AG 339880 Eco_MoM to M.S.M.J., A.V.). S.G.C. was supported by STW grant 13178. Peat soil research was further supported by the Dutch waterboard 'Waternet' (to J.M.H.D., L.P.M.L., and A.J.P.S.)

Appendix A. Supplementary data

Supplementary data to this article can be found online at https://doi.org/10.1016/j.soilbio.2020.107862.

References

Oksanen, A.J., Blanchet, F.G., Friendly, M., Kindt, R., Legendre, P., Mcglinn, D., et al., 2018. Vegan: community ecology package. https://CRAN.R-Project.Org/Package=vegan.

Aromokeye, D.A., Richter-Heitmann, T., Oni, O.E., Kulkarni, A., Yin, X., Kasten, S., et al., 2018. Temperature controls crystalline iron oxide utilization by microbial communities in methanic ferruginous marine sediment incubations. Frontiers in Microbiology 9, 2574. https://doi.org/10.3389/fmicb.2018.02574.

Baird, A.J., Belyea, L.R., Morris, P.J., 2013. Upscaling of peatland-atmosphere fluxes of methane: small-scale heterogeneity in process rates and the pitfalls of "Bucket-and-Slab" models. In: Baird, Andrew J., Belyea, L.R., Comas, X., Reeve, A.S., Slater, L.D. (Eds.), Carbon Cycling in Northern Peatlands. American Geophysical Union, Washington, DC, pp. 37–53. https://doi.org/10.1029/2008GM000826.

Beare, M.H., Gregorich, E.G., St-Georges, P., 2009. Compaction effects on CO_2 and N_2O production during drying and rewetting of soil. Soil Biology and Biochemistry 41, 611–621. https://doi.org/10.1016/j.soilbio.2008.12.024.

Beetz, S., Liebersbach, H., Glatzel, S., Jurasinski, G., Buczko, U., Höper, H., 2013. Effects of land use intensity on the full greenhouse gas balance in an Atlantic peat bog. Biogeosciences 10, 1067–1082. https://doi.org/10.5194/bg-10-1067-2013.

Bhattacharjee, A.S., Motlagh, A.M., Jetten, M.S.M., Goel, R., 2016. Methane dependent denitrification- from ecosystem to laboratory-scale enrichment for engineering applications. Water Research 99, 244–252. https://doi.org/10.1016/j.watres.2016.04.070.

Blothe, M., Roden, E.E., 2009. Composition and activity of an autotrophic Fe(II)-oxidizing, nitrate-reducing enrichment culture. Applied and Environmental Microbiology 75, 6937–6940. https://doi.org/10.1128/AEM.01742-09.

Bodegom, P.M., Scholten, J.C.M., Stams, A.J.M., 2004. Direct inhibition of methanogenesis by ferric iron. FEMS Microbiology Ecology 49, 261–268. https://doi.org/10.1016/j.femsec.2004.03.017.

Boetius, A., Ferdelman, T., Lochte, K., 2000. Bacterial activity in sediments of the deep Arabian Sea in relation to vertical flux. Deep Sea Research Part II: Topical Studies in Oceanography 47, 2835–2875. https://doi.org/10.1016/S0967-0645(00)00051-5.

Böhm, J., 1925. Über Aluminium- und Eisenhydroxyde. I. Zeitschrift für Anorganische und Allgemeine Chemie 149, 203–216. https://doi.org/10.1002/zaac.19251490114.

Brauer, S.L., Cadillo-Quiroz, H., Ward, R.J., Yavitt, J.B., Zinder, S.H., 2011. *Methanoregula boonei* gen. nov., sp. nov., an acidiphilic methanogen isolated from an acidic peat bog. International Journal of Systematic and Evolutionary Microbiology 61, 45–52. https://doi.org/10.1099/ijs.0.021782-0.

Caccavo, F., Lonergan, D.J., Lovley, D.R., Davis, M., Stolz, J.F., McInerney, M.J., 1994. *Geobacter sulfurreducens* sp. nov., a hydrogen- and acetate-oxidizing dissimilatory metal-reducing microorganism. Applied and Environmental Microbiology 60, 3752–3759.

Cai, C., Leu, A.O., Xie, G.-J., Guo, J., Feng, Y., Zhao, J.-X., et al., 2018. A methanotrophic archaeon couples anaerobic oxidation of methane to Fe(III) reduction. The ISME Journal 12, 1929. https://doi.org/10.1038/s41396-018-0109-x.

Callahan, B.J., McMurdie, P.J., Rosen, M.J., Han, A.W., Johnson, A.J.A., Holmes, S.P., 2016. DADA2: high-resolution sample inference from Illumina amplicon data. Nature Methods 13, 581–583. https://doi.org/10.1038/nmeth.3869.

Caporaso, J.G., Lauber, C.L., Walters, W.A., Berg-Lyons, D., Huntley, J., Fierer, N., et al., 2012. Ultra-high-throughput microbial community analysis on the Illumina HiSeq and MiSeq platforms. The ISME Journal 6, 1621–1624. https://doi.org/10.1038/ismej.2012.8.

Carlson, H.K., Clark, I.C., Blazewicz, S.J., Iavarone, A.T., Coates, J.D., 2013. Fe(II) oxidation is an innate capability of nitrate-reducing Bacteria that involves abiotic and biotic reactions. Journal of Bacteriology 195, 3260–3268. https://doi.org/10.1128/JB.00058-13.

Chang, Y.H., Cheng, T.W., Lai, W.J., Tsai, W.Y., Sun, C.H., Lin, L.H., et al., 2012. Microbial methane cycling in a terrestrial mud volcano in eastern Taiwan. Environmental Microbiology 14, 895–908. https://doi.org/10.1111/j.1462-2920.2011.02658.x.

Chidthaisong, A., 2000. Turnover of glucose and acetate coupled to reduction of nitrate, ferric iron and sulfate and to methanogenesis in anoxic rice field soil. FEMS Microbiology Ecology 31, 73–86. https://doi.org/10.1016/S0168-6496(99)00083-5.

Childs, C.W., 1992. Ferrihydrite: a review of structure, properties and occurrence in relation to soils. Zeitschrift für Pflanzenernährung und Bodenkunde 155, 441–448. https://doi.org/10.1002/jpln.19921550515.

Cornell, R.M., Schwertmann, U., 2003. The Iron Oxides: Structure, Properties, Reactions, Occurrences and Uses, second ed. Wiley, Weinheim, Germany. https://doi.org/10.1002/3527602097.

Couwenberg, J., 2009. Emission factors for managed peat soils (organic soils, histosols): an analysis of IPCC default values. Wetlands International 1, 1–14.

Crowe, S.A., Katsev, S., Leslie, K., Sturm, A., Magen, C., Nomosatryo, S., et al., 2011. The methane cycle in ferruginous Lake Matano. Geobiology 9, 61–78. https://doi.org/10.1111/j.1472-4669.2010.00257.x.

Cruz Viggi, C., Rossetti, S., Fazi, S., Paiano, P., Majone, M., Aulenta, F., 2014. Magnetite particles triggering a faster and more robust syntrophic pathway of methanogenic propionate degradation. Environmental Science and Technology 48, 7536–7543. https://doi.org/10.1021/es5016789.

Dean, J.F., Middelburg, J.J., Röckmann, T., Aerts, R., Blauw, L.G., Egger, M., et al., 2018. Methane feedbacks to the global climate system in a warmer world. Reviews of Geophysics 56, 1–44. https://doi.org/10.1002/2017RG000559.

Egger, M., Rasigraf, O., Sapart, C.J., Jilbert, T., Jetten, M.S.M., Röckmann, T., et al., 2015. Iron-mediated anaerobic oxidation of methane in brackish coastal sediments. Environmental Science and Technology 49, 277–283. https://doi.org/10.1021/es503663z.

Ehrenberg, C.G., 1836. Vorläufige mittheilungen über das wirkliche vorkommen fossiler infusorien und ihre grosse verbreitung. Annalen der Physik 38, 213–227. https://doi.org/10.1002/andp.18361140520.

Emsens, W.-J., Aggenbach, C.J.S., Schoutens, K., Smolders, A.J.P., Zak, D., van Diggelen, R., 2016. Soil iron content as a predictor of carbon and nutrient mobilization in rewetted fens. PloS One 11, e0153166. https://doi.org/10.1371/journal.pone.0153166.

Enwall, K., Philippot, L., Hallin, S., 2005. Activity and composition of the denitrifying bacterial community respond differently to long-term fertilization. Applied and Environmental Microbiology 71, 8335–8343. https://doi.org/10.1128/AEM.71.12.8335-8343.2005.

Ettwig, K.F., Butler, M.K., Le Paslier, D., Pelletier, E., Mangenot, S., Kuypers, M.M.M., et al., 2010. Nitrite-driven anaerobic methane oxidation by oxygenic bacteria. Nature 464, 543–548. https://doi.org/10.1038/nature08883.

Ettwig, K.F., Zhu, B., Speth, D., Keltjens, J.T., Jetten, M.S.M., Kartal, B., 2016. Archaea catalyze iron-dependent anaerobic oxidation of methane. Proceedings of the National Academy of Sciences of the United States of America 113, 12792–12796. https://doi.org/10.1073/pnas.1609534113.

Felgate, H., Giannopoulos, G., Sullivan, M.J., Gates, A.J., Clarke, T.A., Baggs, E., et al., 2012. The impact of copper, nitrate and carbon status on the emission of nitrous oxide by two species of bacteria with biochemically distinct denitrification pathways. Environmental Microbiology 14, 1788–1800. https://doi.org/10.1111/j.1462-2920.2012.02789.x.

Franz, D., Koebsch, F., Larmanou, E., Augustin, J., Sachs, T., 2016. High net CO_2 and CH_4 release at a eutrophic shallow lake on a formerly drained fen. Biogeosciences 13, 3051–3070. https://doi.org/10.5194/bg-13-3051-2016.

Geurts, J.J.M., Van Duinen, G.-J.A., Van Belle, J., Wichmann, S., Wichtmann, W., Fritz, C., 2019. Recognize the high potential of paludiculture on rewetted peat soils to mitigate climate change. Landbauforsh J Sustainable Organic Agric Syst 69, 5–8. https://doi.org/10.3220/LBF1576769203000.

Grabb, K.C., Buchwald, C., Hansel, C.M., Wankel, S.D., 2017. A dual nitrite isotopic investigation of chemodenitrification by mineral-associated Fe(II) and its production of nitrous oxide. Geochimica et Cosmochimica Acta 196, 388–402. https://doi.org/10.1016/j.gca.2016.10.026.

Griess-Romijn van Eck, E., 1996. Physiological and chemical tests for drinking water. Journal of Comparative & Physiological Psychology. NEN 1056 Iv-2 Nederlands Normalisatie Instituut: Rijswijk, The Netherlands.

Günther, A., Barthelmes, A., Huth, V., Joosten, H., Jurasinski, G., Koebsch, F., et al., 2019. Prompt rewetting of drained peatlands reduces climate warming despite methane emissions. BioRxiv. https://doi.org/10.1101/748830, 748830.

Hahn, J., Köhler, S., Glatzel, S., Jurasinski, G., 2015. Methane exchange in a coastal fen in the first year after flooding - a systems shift. PloS One 10, e0140657. https://doi.org/10.1371/journal.pone.0140657.

Haroon, M.F., Hu, S., Shi, Y., Imelfort, M., Keller, J., Hugenholtz, P., et al., 2013. Anaerobic oxidation of methane coupled to nitrate reduction in a novel archaeal lineage. Nature 500, 567–570. https://doi.org/10.1038/nature12375.

Harpenslager, S.F., van den Elzen, E., Kox, M.A.R., Smolders, A.J.P., Ettwig, K.F., Lamers, L.P.M., 2015. Rewetting former agricultural peatlands: topsoil removal as a prerequisite to avoid strong nutrient and greenhouse gas emissions. Ecological Engineering 84, 159–168. https://doi.org/10.1016/j.ecoleng.2015.08.002.

Harrison-Kirk, T., Beare, M.H., Meenken, E.D., Condron, L.M., 2013. Soil organic matter and texture affect responses to dry/wet cycles: effects on carbon dioxide and nitrous oxide emissions. Soil Biology and Biochemistry 57, 43–55. https://doi.org/10.1016/j.soilbio.2012.10.008.

He, S., Tominski, C., Kappler, A., Behrens, S., Roden, E.E., 2016. Metagenomic analyses of the autotrophic Fe(II)-oxidizing, nitrate-reducing enrichment culture KS. Applied and Environmental Microbiology 82, 2656–2668. https://doi.org/10.1128/AEM.03493-15.

Hedrich, S., Schlomann, M., Johnson, D.B., 2011. The iron-oxidizing proteobacteria. Microbiology 157, 1551–1564. https://doi.org/10.1099/mic.0.045344-0.

Heil, J., Wolf, B., Brüggemann, N., Emmenegger, L., Tuzson, B., Vereecken, H., et al., 2014. Site-specific ^{15}N isotopic signatures of abiotically produced N_2O. Geochimica et Cosmochimica Acta 139, 72–82. https://doi.org/10.1016/j.gca.2014.04.037.

Hemes, K.S., Chamberlain, S.D., Eichelmann, E., Knox, S.H., Baldocchi, D.D., 2018. A biogeochemical compromise: the high methane cost of sequestering carbon in restored wetlands. Geophysical Research Letters 45, 6081–6091. https://doi.org/10.1029/2018GL077747.

Herlemann, D.P., Labrenz, M., Jürgens, K., Bertilsson, S., Waniek, J.J., Andersson, A.F., 2011. Transitions in bacterial communities along the 2000 km salinity gradient of the Baltic Sea. The ISME Journal 5, 1571–1579. https://doi.org/10.1038/ismej.2011.41.

Holtan-Hartwig, L., Dörsch, P., Bakken, L.R., 2000. Comparison of denitrifying communities in organic soils: kinetics of NO_3 and N_2O reduction. Soil Biology and Biochemistry 32, 833–844. https://doi.org/10.1016/S0038-0717(99)00213-8.

Jäckel, U., Schnell, S., 2000. Suppression of methane emission from rice paddies by ferric iron fertilization. Soil Biology and Biochemistry 32, 1811–1814. https://doi.org/10.1016/S0038-0717(00)00094-8.

Jetten, M.S.M., Stams, A.J.M., Zehnder, A.J.B., 1992. Methanogenesis from acetate: a comparison of the acetate metabolism in *Methanothrix soehngenii* and M*ethanosarcina* spp. FEMS Microbiology Letters 88, 181–197. https://doi.org/10.1016/0378-1097(92)90802-U.

Jones, L.C., Peters, B., Lezama Pacheco, J.S., Casciotti, K.L., Fendorf, S., 2015. Stable isotopes and iron oxide mineral products as markers of chemodenitrification. Environmental Science and Technology 49, 3444–3452. https://doi.org/10.1021/es504862x.

Joosten, H., 2010. The global peatland CO_2 picture peatland status and drainage related emissions in all countries of the world. Wetlands International 1, 1–10. https://doi.org/10.1137/S1064827501399006.

Joosten, H., Clarke, D., 2002. Wise Use of Mires and Peatlands -Background and Principles Including a Framework for Decision-Making. International Mire Conservation Group and International Peat Society. International Mire Conservation Group, Totnes.

Joosten, H., Sirin, A., Couwenberg, J., Laine, A., Smith, P., 2016. Peatland Restoration and Ecosystem Services. Cambridge University Press, Cambridge. https://doi.org/10.1017/CBO9781139177788.

Juottonen, H., Hynninen, A., Nieminen, M., Tuomivirta, T.T., Tuittila, E.-S., Nousiainen, H., et al., 2012. Methane-cycling microbial communities and methane emission in natural and restored peatlands. Applied and Environmental Microbiology 78, 6386–6389. https://doi.org/10.1128/AEM.00261-12.

Kanaparthi, D., Pommerenke, B., Casper, P., Dumont, M.G., 2013. Chemolithotrophic nitrate-dependent Fe(II)-oxidizing nature of actinobacterial subdivision lineage TM3. The ISME Journal 7, 1582–1594. https://doi.org/10.1038/ismej.2013.38.

Kato, S., Igarashi, K., 2019. Enhancement of methanogenesis by electric syntrophy with biogenic iron-sulfide minerals. MicrobiologyOpen 8, e00647. https://doi.org/10.1002/mbo3.647.

Kato, S., Hashimoto, K., Watanabe, K., 2012. Methanogenesis facilitated by electric syntrophy via (semi)conductive iron-oxide minerals. Environmental Microbiology 14, 1646–1654. https://doi.org/10.1111/j.1462-2920.2011.02611.x.

Kiskira, K., Papirio, S., van Hullebusch, E.D., Esposito, G., 2017. Fe(II)-mediated autotrophic denitrification: a new bioprocess for iron bioprecipitation/biorecovery and simultaneous treatment of nitrate-containing wastewaters. International Biodeterioration & Biodegradation 119, 631–648. https://doi.org/10.1016/j.ibiod.2016.09.020.

Klüber, H., Conrad, R., 1998a. Effects of nitrate, nitrite, NO and N_2O on methanogenesis and other redox processes in anoxic rice field soil. FEMS Microbiology Ecology 25, 301–319. https://doi.org/10.1016/S0168-6496(98)00011-7.

Klüber, H., Conrad, R., 1998b. Inhibitory effects of nitrate, nitrite, NO and N_2O on methanogenesis by *Methanosarcina barkeri* and *Methanobacterium bryantii.* FEMS Microbiology Ecology 25, 331–339. https://doi.org/10.1016/S0168-6496(97)00102-5.

Knox, S.H., Sturtevant, C., Matthes, J.H., Koteen, L., Verfaillie, J., Baldocchi, D., 2015. Agricultural peatland restoration: effects of land-use change on greenhouse gas (CO_2 and CH_4) fluxes in the Sacramento-San Joaquin Delta. Global Change Biology 21, 750–765. https://doi.org/10.1111/gcb.12745.

Kostka, J.E., Green, S.J., Rishishwar, L., Prakash, O., Katz, L.S., Marino-Ramirez, L., et al., 2012. Genome sequences for six *Rhodanobacter* strains, isolated from soils and the terrestrial subsurface, with variable denitrification capabilities. Journal of Bacteriology 194, 4461–4462. https://doi.org/10.1128/JB.00871-12.

Kotsyurbenko, O.R., Nozhevnikova, A.N., Zavarzin, G.A., 1993. Methanogenic degradation of organic matter by anaerobic bacteria at low temperature. Chemosphere 27, 1745–1761. https://doi.org/10.1016/0045-6535(93)90155-X.

Lamers, L.P.M., Smolders, A.J.P., Roelofs, J.G.M., 2002. The restoration of fens in The Netherlands. Hydrobiologia 478, 107–130. https://doi.org/10.1023/A:1021022529475.

Lamers, L.P.M., Vile, M.A., Grootjans, A.P., Acreman, M.C., van Diggelen, R., Evans, M. G., et al., 2015. Ecological restoration of rich fens in Europe and North America: from trial and error to an evidence-based approach. Biological Reviews of the Cambridge Philosophical Society 90, 182–203. https://doi.org/10.1111/brv.12102.

Leibl, H., Tomasits, R., Brühl, P., Kerschbaum, A., Eibl, M.M., Mannhalter, J.W., 1999. Humoral and cellular immunity induced by antigens adjuvanted with colloidal iron hydroxide. Vaccine 17, 1017–1023. https://doi.org/10.1016/S0264-410X(98)00201-1.

Leifeld, J., Müller, M., Fuhrer, J., 2011. Peatland subsidence and carbon loss from drained temperate fens. Soil Use & Management 27, 170–176. https://doi.org/10.1111/j.1475-2743.2011.00327.x.

Li, H., Chang, J., Liu, P., Fu, L., Ding, D., Lu, Y., 2015. Direct interspecies electron transfer accelerates syntrophic oxidation of butyrate in paddy soil enrichments. Environmental Microbiology 17, 1533–1547. https://doi.org/10.1111/1462-2920.12576.

Liu, D., Dong, H., Bishop, M.E., Wang, H., Agrawal, A., Tritschler, S., et al., 2011. Reduction of structural Fe(III) in nontronite by methanogen *Methanosarcina barkeri*. Geochimica et Cosmochimica Acta 75, 1057–1071. https://doi.org/10.1016/j.gca.2010.11.009.

Liu, S., Schloter, M., Brüggemann, N., 2018. Accumulation of NO_2^- during periods of drying stimulates soil N_2O emissions during subsequent rewetting. European Journal of Soil Science 69, 936–946. https://doi.org/10.1111/ejss.12683.

Lovley, D.R., Phillips, E.J., 1986. Availability of ferric iron for microbial reduction in bottom sediments of the freshwater tidal potomac river. Applied and Environmental Microbiology 52, 751–757.

Lovley, D.R., Dwyer, D.F., Klug, M.J., 1982. Kinetic analysis of competition between sulfate reducers and methanogens for hydrogen in sediments. Applied and Environmental Microbiology 43, 1373–1379.

Lovley, D.R., Phillips, E.J.P., Lonergan, D.J., 1991. Enzymic versus nonenzymic mechanisms for iron(III) reduction in aquatic sediments. Environmental Science and Technology 25, 1062–1067. https://doi.org/10.1021/es00018a007.

Lovley, D.R., Giovannoni, S.J., White, D.C., Champine, J.E., Phillips, E.J.P., Gorby, Y.A., et al., 1993. *Geobacter metallireducens* gen. nov. sp. nov., a microorganism capable of coupling the complete oxidation of organic compounds to the reduction of iron and other metals. Archives of Microbiology 159, 336–344. https://doi.org/10.1007/BF00290916.

Lovley, D.R., Holmes, D.E., Nevin, K.P., 2004. Dissimilatory Fe(III) and Mn(IV) reduction. Advances in Microbial Physiology 49, 219–286. https://doi.org/10.1016/S0065-2911(04)49005-5.

Marquart, K.A., Haller, B.R., Paper, J.M., Flynn, T.M., Boyanov, M.I., Shodunke, G., et al., 2019. Influence of pH on the balance between methanogenesis and iron reduction. Geobiology 17, 185–198. https://doi.org/10.1111/gbi.12320.

McMurdie, P.J., Holmes, S., 2013. Phyloseq: an R package for reproducible interactive analysis and graphics of microbiome census data. PloS One 8, e61217. https://doi.org/10.1371/journal.pone.0061217.

Milucka, J., Ferdelman, T.G., Polerecky, L., Franzke, D., Wegener, G., Schmid, M., et al., 2012. Zero-valent sulphur is a key intermediate in marine methane oxidation. Nature 491, 541–546. https://doi.org/10.1038/nature11656.

Miranda, K.M., Espey, M.G., Wink, D.A., 2001. A rapid, simple spectrophotometric method for simultaneous detection of nitrate and nitrite. Nitric Oxide 5, 62–71. https://doi.org/10.1006/niox.2000.0319.

Mohamed Abdalla, C., Abdalla, M., Hastings, A., Truu, J., Espenberg, M., Mander, Ü., et al., 2016. Emissions of methane from northern peatlands: a review of management impacts and implications for future management options. Ecology and Evolution 6, 7080–7102. https://doi.org/10.1002/ece3.2469.

Myhre, G., Shindell, D., Bréon, F.-M., Collins, W., Fuglestvedt, J., Huang, J., et al., 2013. Anthropogenic and natural radiative forcing. In: Stocker, T., Qin, D., Plattner, G., Tignor, M., Allen, S., Boschung, J., et al. (Eds.), Climate Change 2013: the Physical Science Basis. Contribution of Working Group I to the Fifth Assessment Report of the Intergovernmental Panel on Climate Change. Cambridge University Press, Cambridge, United Kingdom and New York, NY, USA, pp. 659–740. https://doi.org/10.1017/CBO9781107415324.018.

Nordhoff, M., Tominski, C., Halama, M., Byrne, J.M., Obst, M., Kleindienst, S., et al., 2017. Insights into nitrate-reducing Fe(II) oxidation mechanisms through analysis of cell-mineral associations, cell encrustation, and mineralogy in the chemolithoautotrophic enrichment culture KS. Applied and Environmental Microbiology 83. https://doi.org/10.1128/AEM.00752-17 e00752-17.

Parks, D.H., Rinke, C., Chuvochina, M., Chaumeil, P.-A., Woodcroft, B.J., Evans, P.N., et al., 2017. Recovery of nearly 8,000 metagenome-assembled genomes substantially expands the tree of life. Nature Microbiology 2, 1533–1542. https://doi.org/10.1038/s41564-017-0012-7.

Phillips, E.J.P., Lovley, D.R., Roden, E.E., 1993. Composition of non-microbially reducible Fe(III) in aquatic sediments. Applied and Environmental Microbiology 59, 2727–2729.

Prakash, D., Chauhan, S.S., Ferry, J.G., 2019. Life on the thermodynamic edge: respiratory growth of an acetotrophic methanogen. Science Advances 5, eaaw9059. https://doi.org/10.1126/sciadv.aaw9059.

Qu, D., Ratering, S., Schnell, S., 2004. Microbial reduction of weakly crystalline Iron (III) oxides and suppression of methanogenesis in paddy soil. Bulletin of Environmental Contamination and Toxicology 72, 1172–1181. https://doi.org/10.1007/s00128-004-0367-3.

Raghoebarsing, A.A., Pol, A., van de Pas-Schoonen, K.T., Smolders, A.J.P., Ettwig, K.F., Rijpstra, W.I.C., et al., 2006. A microbial consortium couples anaerobic methane oxidation to denitrification. Nature 440, 918–921. https://doi.org/10.1038/nature04617.

Rotaru, A.-E., Shrestha, P.M., Liu, F., Shrestha, M., Shrestha, D., Embree, M., et al., 2014. A new model for electron flow during anaerobic digestion: direct interspecies electron transfer to *Methanosaeta* for the reduction of carbon dioxide to methane. Energy & Environmental Science 7, 408–415. https://doi.org/10.1039/C3EE42189A.

Roy, R., Conrad, R., 1999. Effect of methanogenic precursors (acetate, hydrogen, propionate) on the suppression of methane production by nitrate in anoxic rice field soil. FEMS Microbiology Ecology 28, 49–61. https://doi.org/10.1016/S0168-6496(98)00092-0.

RStudio Team, 2015. Rstudio: integrated development for R. URL. https://Rstudio.Com.

Rudaz, A.O., Davidson, E.A., Firestone, M.K., 1991. Sources of nitrous oxide production following wetting of dry soil. FEMS Microbiology Letters 85, 117–124. https://doi.org/10.1111/j.1574-6968.1991.tb04703.x-i1.

Ruser, R., Flessa, H., Russow, R., Schmidt, G., Buegger, F., Munch, J.C., 2006. Emission of N_2O, N_2 and CO_2 from soil fertilized with nitrate: effect of compaction, soil moisture and rewetting. Soil Biology and Biochemistry 38, 263–274. https://doi.org/10.1016/j.soilbio.2005.05.005.

Samaritani, E., Siegenthaler, A., Yli-Petäys, M., Buttler, A., Christin, P.-A., Mitchell, E.A. D., 2011. Seasonal net ecosystem carbon exchange of a regenerating cutaway bog: how long does it take to restore the C-sequestration function? Restoration Ecology 19, 480–489. https://doi.org/10.1111/j.1526-100X.2010.00662.x.

Saunois, M., Bousquet, P., Poulter, B., Peregon, A., Ciais, P., Canadell, J.G., et al., 2016. The global methane budget 2000–2012. Earth System Science Data 8, 697–751. https://doi.org/10.5194/essd-8-697-2016.

Scheller, S., Yu, H., Chadwick, G.L., McGlynn, S.E., Orphan, V.J., 2016. Artificial electron acceptors decouple archaeal methane oxidation from sulfate reduction. Science 351, 703–707. https://doi.org/10.1126/science.aad7154.

Schink, B., 1997. Energetics of syntrophic cooperation in methanogenic degradation. Microbiology and Molecular Biology Reviews: Microbiology and Molecular Biology Reviews 61, 262–280.

Scholten, J.C.M., Stams, A.J.M., 1995. The effect of sulfate and nitrate on methane formation in a freshwater sediment. Antonie van Leeuwenhoek 68, 309–315. https://doi.org/10.1007/BF00874141.

Schwertmann, U., Cornell, R.M., 1991. Iron Oxides in the Laboratory. Preparation and Characterization, second ed. WILEY-VCH Verlag, Weinheim, Germany.

Semrau, J.D., DiSpirito, A.A., Yoon, S., 2010. Methanotrophs and copper. FEMS Microbiology Reviews 34, 496–531. https://doi.org/10.1111/j.1574-6976.2010.00212.x.

Smolders, A.J.P., Lamers, L.P.M., Lucassen, E.C.H.E.T., Van Der Velde, G., Roelofs, J.G. M., 2006. Internal eutrophication: how it works and what to do about it - a review. Chemistry and Ecology 22, 93–111. https://doi.org/10.1080/02757540600579730.

Snider, D., Thompson, K., Wagner-Riddle, C., Spoelstra, J., Dunfield, K., 2015. Molecular techniques and stable isotope ratios at natural abundance give complementary inferences about N_2O production pathways in an agricultural soil following a rainfall event. Soil Biology and Biochemistry 88, 197–213. https://doi.org/10.1016/j.soilbio.2015.05.021.

Strack, M., Zuback, Y.C.A., 2013. Annual carbon balance of a peatland 10 yr following restoration. Biogeosciences 10, 2885–2896. https://doi.org/10.5194/bg-10-2885-2013.

Straub, K.L., Benz, M., Schink, B., Widdel, F., 1996. Anaerobic, nitrate-dependent microbial oxidation of ferrous iron. Applied and Environmental Microbiology 62, 1458–1460.

Straub, K.L., Schönhuber, W.A., Buchholz-Cleven, B.E.E., Schink, B., 2004. Diversity of ferrous iron-oxidizing, nitrate-reducing Bacteria and their involvement in oxygen-independent iron cycling. Geomicrobiology Journal 21, 371–378. https://doi.org/10.1080/01490450490485854.

Syvitski, J.P.M., Kettner, A.J., Overeem, I., Hutton, E.W.H., Hannon, M.T., Brakenridge, G.R., et al., 2009. Sinking deltas due to human activities. Nature Geoscience 2, 681–686. https://doi.org/10.1038/ngeo629.

Takai, K., Horikoshi, K., 2000. Rapid detection and quantification of members of the archaeal community by quantitative PCR using fluorogenic probes. Applied and Environmental Microbiology 66, 5066–5072. https://doi.org/10.1128/AEM.66.11.5066-5072.2000.

Tang, J., Zhuang, L., Ma, J., Tang, Z., Yu, Z., Zhou, S., 2016. Secondary mineralization of ferrihydrite affects microbial methanogenesis in *Geobacter-Methanosarcina* cocultures. Applied and Environmental Microbiology 82, 5869–5877. https://doi.org/10.1128/AEM.01517-16.

Teh, Y.A., Dubinsky, E.A., Silver, W.L., Carlson, C.M., 2007. Suppression of methanogenesis by dissimilatory Fe(III)-reducing bacteria in tropical rain forest soils: implications for ecosystem methane flux. Global Change Biology 14, 413–422. https://doi.org/10.1111/j.1365-2486.2007.01487.x.

Timmers, P.H.A., Welte, C.U., Koehorst, J.J., Plugge, C.M., Jetten, M.S.M., Stams, A.J.M., 2017. Reverse methanogenesis and respiration in methanotrophic archaea. Archaea 1–22. https://doi.org/10.1155/2017/1654237, 2017.

Torres, N.T., Och, L.M., Hauser, P.C., Furrer, G., Brandl, H., Vologina, E., et al., 2014. Early diagenetic processes generate iron and manganese oxide layers in the sediments of Lake Baikal, Siberia. Environmental Sciences: Processes & Impacts 16, 879–889. https://doi.org/10.1039/c3em00676j.

Vaksmaa, A., Lüke, C., van Alen, T., Valè, G., Lupotto, E., Jetten, M.S.M., et al., 2016. Distribution and activity of the anaerobic methanotrophic community in a nitrogen-

fertilized Italian paddy soil. FEMS Microbiology Ecology 92, 1–11. https://doi.org/10.1093/femsec/fiw181.

Vaksmaa, A., Guerrero-Cruz, S., van Alen, T.A., Cremers, G., Ettwig, K.F., Lüke, C., et al., 2017. Enrichment of anaerobic nitrate-dependent methanotrophic '*Candidatus* Methanoperedens nitroreducens' archaea from an Italian paddy field soil. Applied Microbiology and Biotechnology 101, 7075–7084. https://doi.org/10.1007/s00253-017-8416-0.

Van Den Heuvel, R.N., Van Der Biezen, E., Jetten, M.S.M., Hefting, M.M., Kartal, B., 2010. Denitrification at pH 4 by a soil-derived *Rhodanobacter*-dominated community. Environmental Microbiology 12, 3264–3271. https://doi.org/10.1111/j.1462-2920.2010.02301.x.

Van Den Heuvel, R.N., Bakker, S.E., Jetten, M.S.M., Hefting, M.M., 2011. Decreased N2O reduction by low soil pH causes high N2O emissions in a riparian ecosystem. Geobiology 9, 294–300. https://doi.org/10.1111/j.1472-4669.2011.00276.x.

Vanselow-Algan, M., Schmidt, S.R., Greven, M., Fiencke, C., Kutzbach, L., Pfeiffer, E.-M., 2015. High methane emissions dominated annual greenhouse gas balances 30 years after bog rewetting. Biogeosciences 12, 4361–4371. https://doi.org/10.5194/bg-12-4361-2015.

Wen, X., Unger, V., Jurasinski, G., Koebsch, F., Horn, F., Rehder, G., et al., 2018. Predominance of methanogens over methanotrophs contributes to high methane emissions in rewetted fens. Biogeosciences 15, 6519–6536. https://doi.org/10.5194/bg-2018-184.

Wickham, H., 2016. ggplot2: Elegant Graphics for Data Analysis. Springer-Verlag, New York.

Wilhelm, E., Battino, R., Wilcock, R.J., 1977. Low-pressure solubility of gases in liquid water. Chemical Reviews 77, 219–262. https://doi.org/10.1021/cr60306a003.

Wilson, D., Alm, J., Laine, J., Byrne, K.A., Farrell, E.P., Tuittila, E.-S., 2009. Rewetting of cutaway peatlands: are we re-creating hot spots of methane emissions? Restoration Ecology 17, 796–806. https://doi.org/10.1111/j.1526-100X.2008.00416.x.

Yamada, C., Kato, S., Kimura, S., Ishii, M., Igarashi, Y., 2014. Reduction of Fe(III) oxides by phylogenetically and physiologically diverse thermophilic methanogens. FEMS Microbiology Ecology 89, 637–645. https://doi.org/10.1111/1574-6941.12365.

Zak, D., Goldhammer, T., Cabezas, A., Gelbrecht, J., Gurke, R., Wagner, C., et al., 2018. Top soil removal reduces water pollution from phosphorus and dissolved organic matter and lowers methane emissions from rewetted peatlands. Journal of Applied Ecology 55, 311–320. https://doi.org/10.1111/1365-2664.12931.

Zhou, S., Xu, J., Yang, G., Zhuang, L., 2014. Methanogenesis affected by the co-occurrence of iron(III) oxides and humic substances. FEMS Microbiology Ecology 88, 107–120. https://doi.org/10.1111/1574-6941.12274.

Zhuang, L., Xu, J., Tang, J., Zhou, S., 2015. Effect of ferrihydrite biomineralization on methanogenesis in an anaerobic incubation from paddy soil. Journal of Geophysical Research: Biogeosciences 120, 876–886. https://doi.org/10.1002/2014JG002893.